Article

DEMSA Protocol: Deterioration Effect Modelling for Structural Assessment of RC Buildings

Elena Casprini [1,*], Chiara Passoni [1], Alessandra Marini [1] and Gianni Bartoli [2]

1 Department of Engineering and Applied Sciences, University of Bergamo, Viale Marconi 5, 24044 Dalmine, Italy; chiara.passoni@unibg.it (C.P.); alessandra.marini@unibg.it (A.M.)
2 Department of Civil and Environmental Engineering, University of Florence, Via di S.Marta 3, 50139 Florence, Italy; gianni.bartoli@unifi.it
* Correspondence: elena.casprini@unibg.it

Abstract: The effects of deterioration strongly impact the expected future service life and the structural performances of existing reinforced concrete structures. Currently, straightforward methodologies are required to include such effects in the assessment and renovation of the RC buildings' heritage. A simplified protocol enabling the detection, evaluation, and modelling of corrosion effects is presented in this paper. The protocol provides the guidance for the design and management of the on-site diagnostic campaign, aimed at identifying a possible corrosion risk scenario. Then, equivalent damage parameters describing corrosion effects in the structural models can be calibrated. Structural performances over time can be assessed to predict the structural residual life, maintenance management criteria and timing, and major indications on the feasibility of the retrofit intervention, or the unavoidable need of demolition. The application of the proposed protocol to some case studies emphasises the effectiveness of the procedure for detecting possible activated corrosion processes and for supporting engineers in their decision-making process and choice of renovation strategy.

Keywords: existing RC structures; deterioration level; corrosion effects; assessment protocol; life-cycle structural performances; durability; retrofit strategy; demolition vs. renovation

1. Introduction

Reinforced concrete (RC) buildings represent a great share of the existing building stock; most of them are obsolete, energy inefficient, and vulnerable to seismic hazards. Thus, innovative retrofit techniques are being developed to address sustainability, safety, and resilience by adopting a comprehensive approach [1]. In this scenario, an underestimated critical aspect is that any RC structure, regardless of its construction period, adopted material, or structural use, may be affected by deterioration processes evolving over time. As a matter of fact, many existing RC buildings present a very poor state of preservation, whilst others may hide potentially harmful deterioration processes.

However, in current renovation practice, the actual level of the deterioration of existing structures is rarely addressed, with the risk of investing in great renovation projects for structures that are seriously deteriorated and/or are expected to be compromised in the near future. The evaluation of the causes and effects of deterioration is usually investigated only in emergency situations for common buildings, when signs of deterioration are clearly visible and structural elements are seriously compromised, e.g., in case of a lack of cover and the presence of exposed corroded rebars. However, the evaluation of the structures' actual state of preservation in their present and future life may be seen as a priority in the great renovation wave that is affecting our building stock. The effects of deterioration and, in particular, corrosion, which has the greatest impacts on structural behaviour [2,3], need to be included in the assessment process to perform an effective modelling of the structural behaviour and to obtain a reliable prediction of performance in the building's as-is and retrofitted conditions over the whole life cycle. In addition, the actual level of deterioration

also affects the choice of the renovation strategy by identifying those structural elements which are no longer able to perform their structural function due to deterioration, and that might require a downgrade of their structural role. The common practice of disregarding the level of deterioration in retrofitting projects may have two main causes: a lack of awareness of the causes and effects of deterioration on RC buildings, and a lack of shared and straightforward scientific tools, allowing for the integration of such evaluations into the structural diagnosis and assessment process. The problem of corrosion in RC structures involves multifaceted aspects which cannot be faced by a single disciplinary field, requiring experience in several sectors such as diagnostics, electrochemistry, materials, and structural engineering (Figure 1).
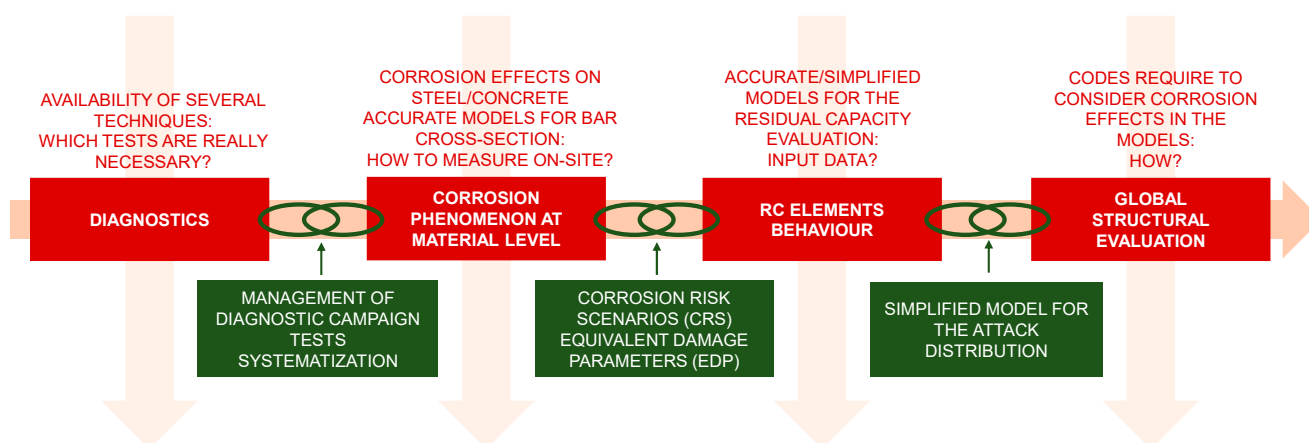
Figure 1. Current practice and state of the art, fragmented into not-interrelated disciplines: major issues inhibiting the modelling of deterioration in current structural analyses (light red arrows, red boxes, and text); identification of required tools to cover the gap between disciplines and to merge them into a new comprehensive approach (green boxes and text).

Despite such a complex scenario, to date, a sectorial approach is often pursued; as a result, while deep and extensive knowledge has been developed in each research field, the applicability of such knowledge may be limited in practice. Considering diagnostics, many techniques are available to evaluate the chemical, physical, or environmental parameters influencing the corrosion process; however, the practitioner engineers may not be aware of which tests are necessary in each case, and the techniques may present some issues limiting their practical applications. For example, electrochemical techniques for the characterisation of the corrosion phenomena require a high level of expertise and are not adequate for single in-field inspections because they need a longer monitoring campaign [4]; or the widely suggested gravimetric method, which consists in estimating the bar cross-section loss by measuring the mass loss on a bar piece, entails the removal of the concrete cover and the extraction of a bar piece in several locations, thus being invasive and not providing information about possible localised attacks in other locations. On the other hand, rapid and non-invasive in-field tests to detect and quantify the amount of chlorides in concrete, which is one of the major causes of corrosion, are still not available. As for material engineering, the level of accuracy to which the corrosion phenomenon is studied at the material level is often not applicable at the scale of the structure. For example, the distribution of the corrosion attack on the section and along the bar length cannot be measured on site for the whole structure; in addition, the parameters influencing the corrosion damage may be highly variable in time and difficult to determine on site. Considering the experimental and analytical studies about the effects of corrosion on single RC elements, in the former, artificial corrosion is usually applied to the elements, which may be not representative of the natural phenomenon; in the latter, too-sophisticated models are usually applied that may not have been extended at the building level for the required high computational effort. Some models enabling the evaluation of residual capacity for single structural elements

have been developed [3,5], but they require the definition of the corrosion level as input data, and straightforward and systematised methods to collect such information in real structures are not currently available. Finally, as for structural engineering, codes and guidelines [6,7] recommend considering the deterioration level in the structural assessment without providing specific guidance. From this brief discussion of the current state of the art, it clearly emerges that cross-contamination among different sectors is fundamental to exploit the available knowledge and define a validated methodological approach to guide the engineers from the on-site structure inspection, to enable the modelling of deterioration effects in the preliminary assessment of both the as-is condition of the structure and the feasibility of retrofit interventions.

In this perspective, the DEMSA protocol (Deterioration Effect Modelling for Structural Assessment protocol) is presented in this paper and is validated against some case studies. The protocol collects and systematises the state of the art in each field, trying to overcome some of the limits to the applicability of those studies in the current renovation practice (Figure 1). The core proposal consists in relating different types of corrosion attacks to easily measurable environmental conditions, grouped into corrosion risk scenarios (CRS). Such classification allows the engineer to plan and manage the diagnostic campaign in a rational and systematised way, based on the hypothesis of the possible presence of a specific corrosion risk scenario, reducing the number of necessary tests and, therefore, time and costs. Some corrosion attack characteristics are defined in relation to each scenario, enabling the calibration of simplified equivalent damage parameters (EDP) to be included in the models for a first estimate of the corrosion effects on the structural behaviour. Since the global structural evaluation also requires the modelling of the corrosion attack pattern along the structural elements, a simplified method to relate natural corrosion patterns to the scenarios and to model the attack distribution is also proposed. Such a simplified and straightforward method can be easily integrated in the traditional diagnosis and assessment process for existing RC structures; furthermore, it may provide relevant information to be used in the innovative and increasingly widespread retrofit design frameworks based on a life cycle thinking approach [8]. These frameworks are aimed at identifying, conceiving, and designing the most sustainable retrofit option under an environmental, social, and economic point of view that considers the entire building life cycle, thus requiring the evaluation of the structural performances of the existing building over time, including deterioration effects.

2. The DEMSA Protocol

A simplified scheme of the protocol is represented in Figure 2. The first step consists in the initial on-site survey for damage detection with a visual inspection, for which an abacus of visible deterioration conditions on RC structures is provided. In the second step, the deterioration risk is identified in relation to the environmental and aggressiveness conditions in which corrosion may occur (herein classified in corrosion risk scenarios—CRS) and the results of slightly destructive instrumental tests; then, in relation to each scenario, equivalent damage parameters (EDP) are calibrated in the third step, describing the quantitative effects of such types of corrosion, thus providing an estimate of the deterioration level. By adopting these parameters, in the fourth step, sensitivity analyses are carried out in order to evaluate the relevance of deterioration effects on the structural behaviour. Finally, the impact on modelling and/or on retrofit strategies is defined as a protocol outcome.
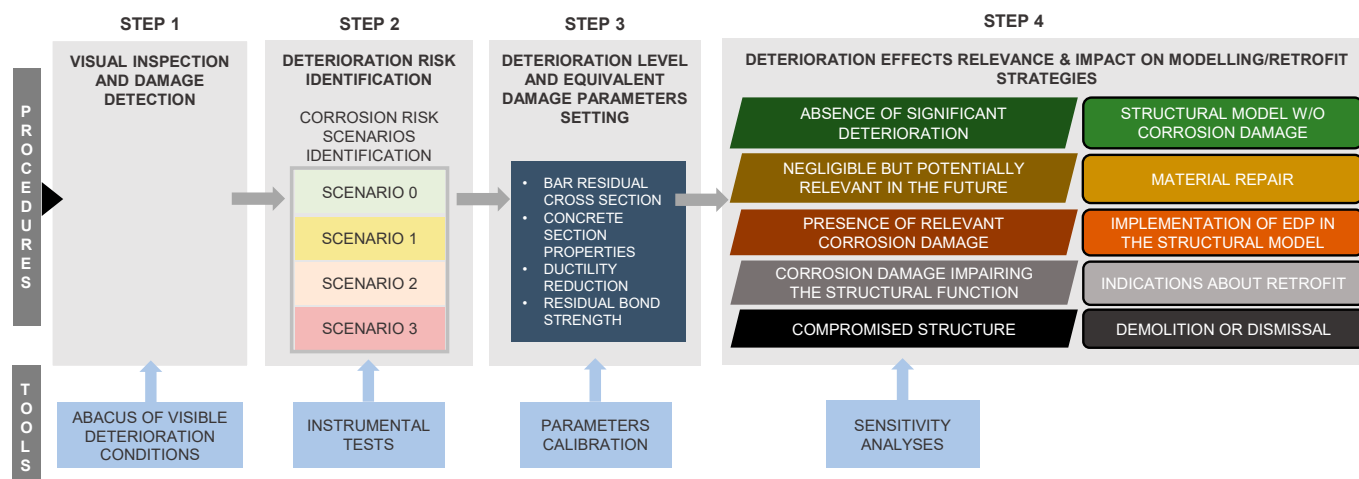
Figure 2. Steps of the DEMSA protocol: (1) visual inspection, (2) definition of the deterioration risk by identifying a corrosion risk scenario (CRS), (3) estimate of the deterioration level by means of equivalent damage parameters (EDP), (4) definition of the deterioration effects' relevance on structures and the actions to be implemented in the structural model/preliminary selection of the renovation strategy.

As shown in Figure 2 (Step 4), the protocol outcomes may provide limit conditions for the structural assessment and retrofit, from the condition of negligible corrosion effects with respect to the structural behaviour (if 'absence of significant deterioration' is obtained, structural modelling can be performed disregarding the risk of corrosion), to the case with a level of deterioration so heavy as to limit the applicability of retrofit solutions (thus, 'demolition or dismissal' should be preferred from a structural point of view). In all the intermediate conditions, the DEMSA protocol allows for a preliminary estimate of the expected corrosion attack type and pattern, and indicates how to consider it in the structural modelling. In some cases, major indications for the preliminary selection of the retrofit intervention may also be derived (in case 'indications about retrofit' is obtained); for example, when some structural elements are heavily compromised and cannot be repaired, all the retrofit solutions relying on those elements should be excluded or re-engineered.

The proposed procedure does not provide an accurate description of the corrosion phenomenon, but it allows for preliminary evaluations of whether the level of deterioration is negligible or significant for the structural behaviour, provides some simple parameters to include deterioration in structural models, and allows one to identify those structures that are eligible for rehabilitation works and those requiring demolition. Furthermore, the protocol promotes a multidisciplinary approach by informing the practitioner engineer of the specialists required for each step of the process.
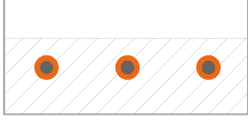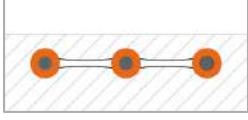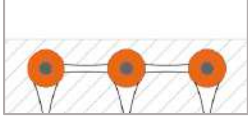
2.1. Step 1—Visual Inspection and Damage Detection

In standard conditions, steel bars embedded in concrete are naturally protected from corrosion due to the high alkalinity of the concrete pore solution originating from concrete hydration (PH around 13). Aggressive substances (mainly carbon dioxide, which produces concrete carbonation, and chloride ions) present in the atmosphere, on the concrete surface, or in the concrete matrix can destroy or locally damage the thin protective oxide film which spontaneously forms on the bar surface (called the passive film), thus depassivating the reinforcement [2]. Then, if the presence of moisture and oxygen at the rebar level occur, the rebar may be subjected to corrosion: metal is transformed into oxides (more commonly rust), leading to both a reduction of the bar cross-section and the expansion of corrosion products, which causes concrete cracking. The rate of the process (expressed as the penetration rate of the corrosion attack in the steel bars and measured in μm/year)

depends on several factors, such as the concrete quality, the moisture content in concrete, and the chloride content.

From a simple representation of the corrosion process (Table 1), it may be noted that, when concrete is apparently sound, the process may be in different stages (ST in the following): absence of aggressive substances (CO_2 and Cl^-) in the concrete cover (ST0); penetration of substances within the cover (ST1); presence of substances at or beyond the rebar level, but absence of conditions activating corrosion (e.g., moisture and oxygen) (ST2); or activated level of corrosion which does not yet result in concrete cracking (ST3). All these stages cannot be detected by visual inspection. In some cases, internal delamination without external cracking (ST4) may occur; therefore, instrumental delamination control [9] should be carried out during the visual inspection in some relevant locations by checking different types of structural elements in different areas. Finally, if corrosion-induced signs of deterioration are visible on the concrete surface, the corrosion process is probably at an advanced stage (ST4 or ST5). The main visible signs of deterioration are described in Tables 2 and 3. Once bars are depassivated and corrosion initiates, corrosion products may migrate through the interconnected pores from the bars to the concrete surface showing rust staining (code A1 in Table 2), or may cause the concrete cracking which first results in external cracks parallel to the reinforcements (A2, A3) and later in the spalling or delamination of concrete cover portions (A4, A5), leading to exposed reinforcements [10]. While conditions grouped into category A refer to signs which are direct consequences of corrosion, attention should be paid also to other deterioration mechanisms (category B in Table 2) or areas exposed to contact with water or high relative humidity (R.H.; category C in Table 2) since, in case of corrosion activation, more relevant corrosion rates may be expected in the affected area. All these visible signs of corrosion-induced deterioration should be checked in the first step of the protocol and noted in a sketch of the structural scheme.

Table 1. Schematic representation of the corrosion stages of steel bars in concrete.

Corrosion Stage	Bars and Concrete Condition	External Evidence
ST0	*Absence of aggressive agents (CO_2 or Cl^-)* Sound concrete Protected bars	
ST1	*Penetration of aggressive agents in the concrete cover* Sound concrete Protected bars	None
ST2	*Aggressive agents at or beyond rebar depth* Sound concrete Unprotected bars	
ST3	*Corrosion initiation* Formation of corrosion products around bars filling concrete pores Sound concrete Corroding bars	None or rust staining
ST4	*Active corrosion* Corrosion product expansion Cracking of concrete Possible delamination Corroding bars	None or swelling or rust staining
ST5	*Active corrosion* Cracking of concrete to the concrete surface Possible spalling Corroding bars	Cracking in connection with main bars and possible rust staining

Table 2. Abacus of the possible visible deterioration conditions.

Code	Condition Detected
category A—Corrosion-induced deterioration	
A1	Rust staining, rust spots
A2	Transversal cracking in correspondence with stirrups
A3	Longitudinal cracking in correspondence with main reinforcing bars
A4	Concrete cover spalling
A5	Concrete cover delamination
category B—Other deterioration mechanisms	
B1	Biological colonisation
B2	Efflorescence
B3	Honeycomb
B4	Cracking or spalling caused by other concrete degradation phenomena
category C—Areas exposed to contact with water or high R.H.	
C1	High R.H. at concrete surface
C2	Wet areas
C3	Water run-off, leakage, infiltration

Since the absence of evident corrosion-induced damage does not necessarily entail the absence of activated corrosion processes [11], it clearly emerges that the risk of corrosion cannot be disregarded based on visual inspections only. One of the main innovative aspects of the DEMSA protocol is, thus, that in the next steps, the procedure would allow detecting the corrosion process also in the early stages by examining the environmental and aggressiveness conditions that may lead to corrosion activation for each structure, regardless of the observed state of preservation.

Table 3. Examples of possible visible deterioration conditions. Signs of damage observed during the inspection in buildings from case studies [12].

A1	A2, A3	A4, A5

B1, B2	B3, B4	C1, C2, C3

### 2.2. Step 2—Corrosion Risk Scenario Identification

The second step of the protocol focuses on the definition of a possible corrosion risk scenario (CRS) for the structural elements, which identifies not only the type of environment in which corrosion may occur, but also the type of attack to which the structure may be subjected in such an environment. The definition of the CRSs proposed in the protocol (Table 4) is based both on the environmental exposure condition and on the possible presence of aggressive conditions on the reinforcement surface that can cause different types of corrosion, such as carbonation or chlorides. According to this new classification, exposure conditions inhibiting corrosion or leading to corrosion attacks with a negligible rate (not significant for the structural performance) are included in Scenario 0, regardless of the type of attack, corresponding to the exposure classes X0, XC1-2-3 of EN 206, 2013 [13]. Environmental conditions leading to carbonation-induced corrosion in absence of chloride with relevant rates are grouped in Scenario 1 (this attack becomes significant only in presence of wet/dry cycles or high R.H.), corresponding to the exposure class XC4 of EN 206. All the exposure conditions leading to chloride-induced corrosion are grouped into one single scenario (Scenario 3), corresponding to the exposure classes XS1, XS3, XD1-2-3 of EN 206. Finally, a further scenario (Scenario 2) is defined, characterised by the simultaneous presence of low chloride content (below chloride threshold for pitting corrosion initiation) in the cementitious matrix and carbonation; the latter may liberate chlorides bound to the hydrated phase, or in the form of calcium chloroaluminate hydrates, making the pore solution even more aggressive. Although, in modern structures, limits are imposed on the chloride content in the cementitious matrix, such a scenario cannot be disregarded since RC elements containing chloride from construction may be found in existing structures [2,14], due to the use of contaminated raw materials (water and aggregates) or due to the addition of accelerant admixtures based on calcium chloride (found in structures built from 1960 to 1980). In this case, corrosion rates become relevant also in moderate humidity conditions (R.H. > 50%), for the hygroscopic nature of chloride-contaminated concrete, which attracts and retains a higher level of moisture [2]. Therefore, Scenario 2 may be associated with environments typical of exposure classes XC3-4 of EN 206.

Table 4. Corrosion risk scenarios for reinforced concrete elements.

Scenario	0	1	2	3
Environmental exposure Exposure classes EN 206, 2013 [13]	Atmospheric Exposure (X0, XC1-2-3)	Atmospheric exposure + wet/dry cycles (XC4)	Atmospheric Exposure (XC3-4)	Infrastructure *and/or* marine exposure *or* industrial brine (XS1, XS3, XD1-2-3)
Presence of aggressive condition on the reinforcement surface	Always saturated by water *or* always dry *or* Non-carbonated w/o chloride *or* Carbonated + R.H. < 70% *or* Chloride (Cl^-) + R.H. < 40%	Carbonated + R.H. > 70%	Carbonated + 0.1% < Cl^- < 0.4% (with respect to cement weight) + R.H. > 50%	Cl^- > 0.4% (with respect to cement weight) + R.H. > 40%

The scenario identification for the structure (or the single structural element) is carried out by progressively examining all those environmental and aggressiveness conditions which may trigger the specific corrosion attack of each scenario (as detailed in the flow chart in Figure 3). After visual inspection and damage detection (black triangle at the top of Figure 3), the possible ingress of chloride from the outside into the concrete is evaluated by collecting information about the surrounding environment. For structures located in marine environments, or when the use of deicing salts or the exposure to aggressive industrial brines is likely to occur, the presence of a chloride penetration profile should be first assessed (necessary tests are described in Table 5); if its presence is detected, Scenario 3

can be directly selected, and the concrete cover should be measured and compared with the chloride penetration depth. If the chloride profile is not found, or if Scenario 3 exposure conditions are excluded a priori, the presence of chloride in the concrete matrix from construction, and the relative chloride content, should be checked in concrete samples from different structural element types, located at different floors. Depending on the chloride content (Cl^- (%)), with respect to the cement weight, different scenarios may be recognised: if $Cl^- > 0.4\%$ [10], the attack is mainly dominated by chlorides and the possibility to have Scenario 3 should be reconsidered, while if $0.1\% < Cl^- \leq 0.4\%$, Scenario 2 is selected. In case $Cl^- \leq 0.1\%$, relevant corrosion rates may be found only for carbonation-induced corrosion in the case of contact with water or very high levels of relative humidity (R.H. $\geq 70\%$); in this case, the structure would be in Scenario 1. Then, the possibility of water leakage or infiltration is examined, and particular attention is paid to those elements which are not sheltered from rain (conditions C from Table 2 detected during visual inspection). If this condition is also excluded for all the structural elements, Scenario 0 can be selected. When either Scenario 1 or 2 is identified for the structure, carbonation depth and concrete cover should be measured and compared (see tests in Table 5), in order to assess whether corrosion is likely to be already active or not.
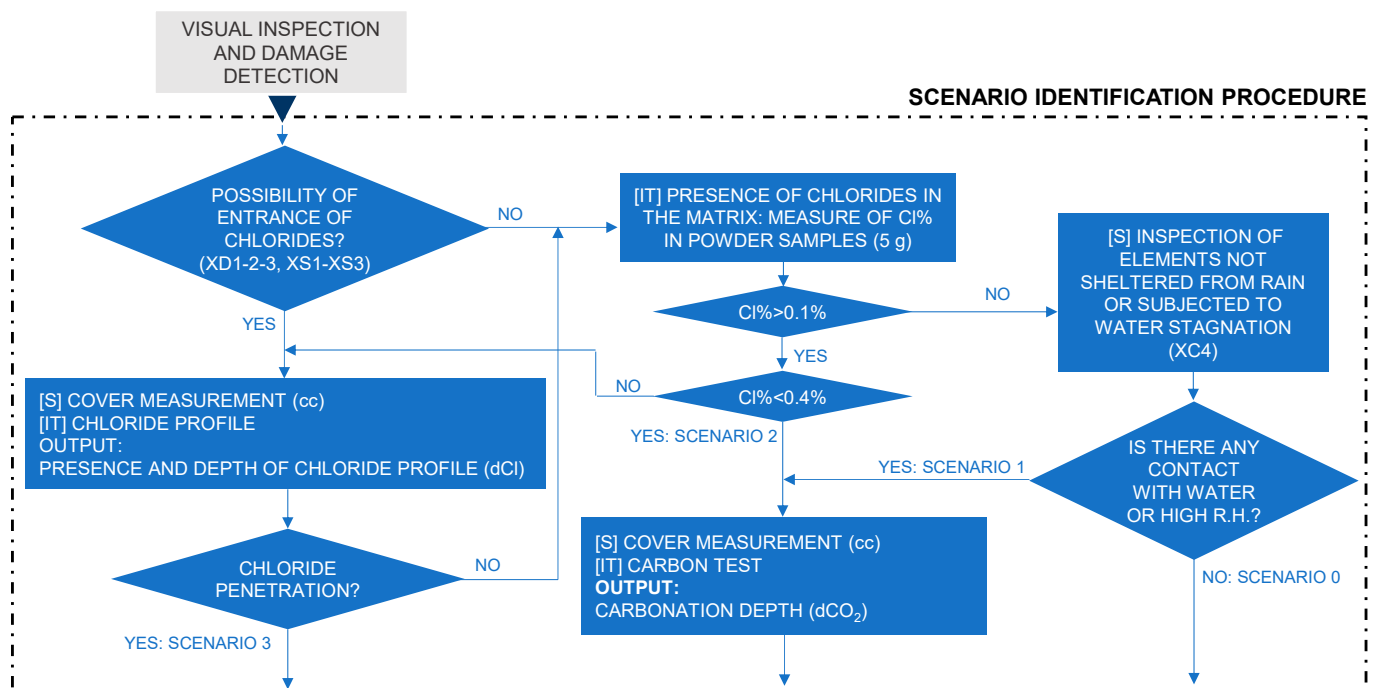
Figure 3. Scenario identification procedure flow chart. (S) refers to surveys and (IT) refers to instrumental tests.

Two critical aspects emerge from this procedure: first, despite that carbonation tests [15,16] are widely performed in current practice to assess the building's state of preservation, they are not significant and may be avoided when Scenarios 0 or 3 are recognised, thereby saving time and costs; secondly, although the presence and content of chloride are the critical information required to identify the actual risk of corrosion and are always necessary, these aspects are often disregarded by practitioner engineers since there are no standardised in-field tests to collect such data. The standardised laboratory method [17] requires collecting concrete powder samples, dispatching them to a chemical laboratory, and waiting for the results for a time of some days; such tests are accurate, but time consuming and costly. An extensive experimental evaluation of four different rapid in-field methods was carried within the Strategic Highway Research Program (SHRP) to evaluate the accuracy of these tests against laboratory methods [18,19]; however, a specific

correlation factor was not found since the correlation is strongly dependent on the chloride content. Further research is thus needed to identify a reliable in-field test; promising preliminary results are shown in Casprini, 2021 [12], by comparing experimental results obtained through laboratory standardised tests and by a commercial titrator conceived for measuring the chloride content in water (Quantab Test Strips® from HACH®), which was adapted for concrete powder.

Table 5. Test required for the scenario identification procedure: description and codes of reference.

Test	Code of Reference	Instructions	Instruments Required
Chloride Content Analysis	EN 14629 [17]	Collect concrete powder samples at the locations of interest and execute chemical laboratory test.	Concrete powder (drill)
Chloride Penetration Depth	EN 14629 [17]	Extract a core or collect concrete powder in separate depth increments from the outer surface to bar level, and execute chemical laboratory tests.	Concrete core or concrete powder (drill or core-drill)
	Collepardi, 1972 [20]	Not codified—spray fluorescein on a freshly broken concrete surface, followed by silver nitrate. Chloride-containing zones turn dark pink, whereas free chloride zones turn dark brown.	Fluorescein (1 g/L in a 70% solution of ethyl alcohol in water) + silver nitrate (0.1 mol/L $AgNO_3$ solution)
Carbonation Depth	EN 14630 [15]	Extract the core or the powder according to the method adopted and spray the indicator phenolphthalein on fresh concrete. Carbonated concrete does not change its colour, while non-carbonated concrete turns purple.	Concrete core + phenolphthalein or CARBONTEST© kit [16]
Concrete Cover Measurement	ACI 222R-19 [9]	Measure concrete cover at different locations to obtain an average value.	Cover meter and/or calibre

2.3. Step 3—Calibration of the Equivalent Damage Parameters

Once a corrosion risk scenario is identified, equivalent damage parameters (EDP) describing the corrosion effects in the structural models are estimated. The procedure adopted to calculate the EDP is presented in Figure 4, and involves three phases: (i) the collection of input data from in situ observations and from the instrumental tests carried out according to the scenario identification procedure (Section 2.3.1); (ii) the definition of the corrosion attack characteristics associated with each scenario (i.e., the average corrosion, the maximum-to-average attack ratio, and the attack model on the bar section and along its length, as described in Section 2.3.2); and (iii) the setting of the equivalent damage parameters through formulations available in the literature (Section 2.3.3). The primary parameters enabling the description of corrosion damage in the structural model are the bar average and minimum residual cross-section, the reduced concrete section properties, and the possible reduction of bond strength and bars ductility.
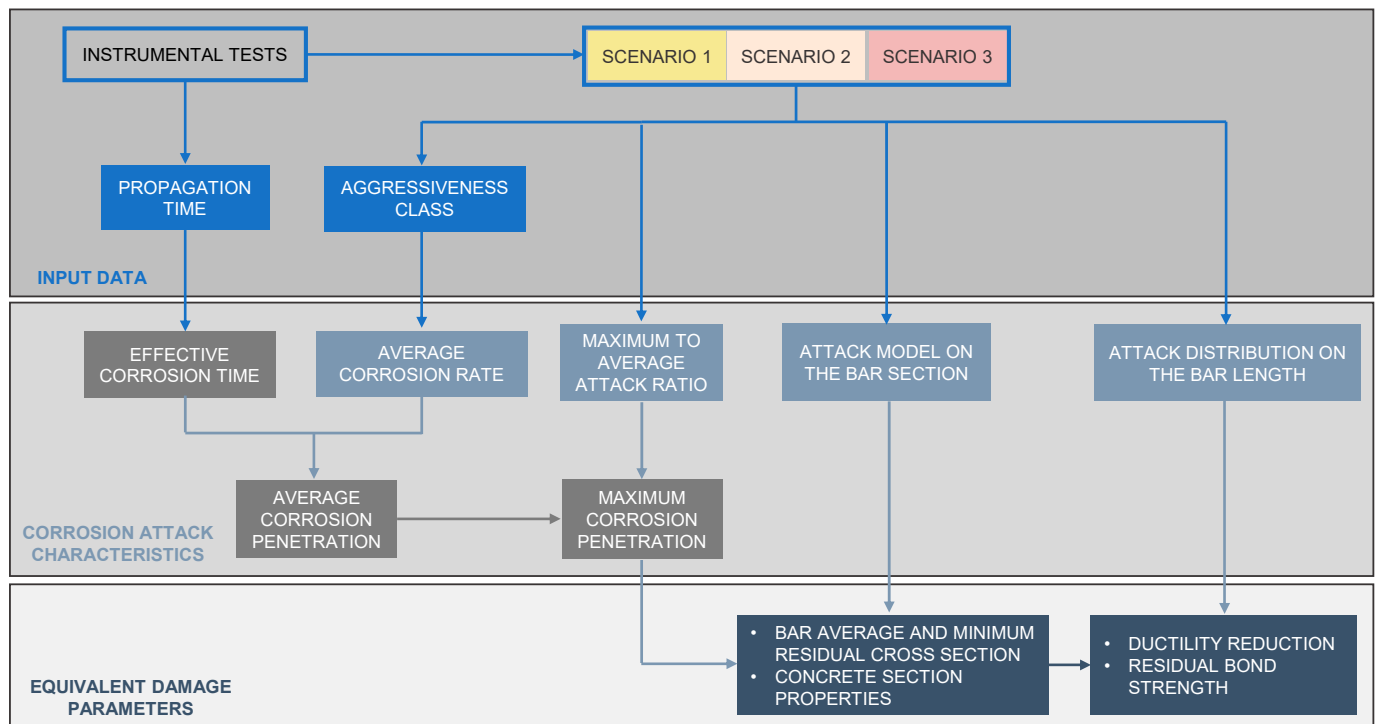
Figure 4. Three-phase process for the definition of the equivalent damage parameters to be implemented in the structural analyses: in blue are the input data; in light blue are the corrosion attack characteristics, selected from the scenarios; in dark blue are the final equivalent damage parameters, and in grey is the information calculated.

2.3.1. Input Data

Fundamental information is required for the calibration of the EDP: the *propagation time* (T_p), here defined as the time frame from bar depassivation to survey, in the case where corrosion is active; or the *time left to corrosion initiation* ($T_{i,l}$), i.e., the time frame from survey to rebar depassivation, which occurs when either the carbonation front or the critical chloride threshold reaches the rebar level, in the case where corrosion may activate in the future.

A simplified approach is adopted in the DEMSA protocol to calculate these significant time periods (as proposed in the CONTECVET manual [4]), which is based on the results of the instrumental tests carried out during the scenario identification procedure (as described in Section 2.2). Firstly, a value for the parameter K (related to the aggressive substance penetration rate and measured in mm/year$^{1/2}$) is estimated in a simplified manner by adopting the square root formula (Equation (1)):

$$K = \frac{d}{\sqrt{t}} = \frac{dCO_2(dCl)}{\sqrt{T_{survey} - T_{0,agg}}} \tag{1}$$

where d is the depth of penetration in mm and is calculated from the measurement of the carbonation dCO_2 (or chloride profile dCl) penetration depth measured on-site, and t is the time in years, which is the difference between the year of survey (T_{survey}) and the time since the aggressive substance started to penetrate from the concrete edge ($T_{0,agg}$), which is known. It should be noted that, although, in general, $T_{0,agg}$ may correspond to the structure's construction year (T_0), in some other cases, environmental aggressiveness conditions may have changed during the structure's life, for example, if an external source of chlorides has been located close to the structure of interest (Scenario 3), or if the structure has always been kept saturated, preventing the carbonation front from penetrating, and then dried (Scenario 1 and 2); moreover, if the concrete cover had been repaired by

removing aggressive substances in past interventions, $T_{0,agg}$ may be assumed as the year of such intervention.

Once the parameter K is defined with Equation (1), which provides an approximate value since K is actually a distribution of values and not a deterministic number, the initiation time (T_i), i.e., the interval of time necessary for the aggressive substances to reach bars with a K since $T_{0,agg}$, is calculated with Equation (2):

$$T_i = \frac{cc^2}{K^2} \tag{2}$$

where cc is the concrete cover dimension. Finally, depending on whether the aggressive substances have (activated corrosion) or have not (possible activation in the future) reached the rebar level, the *propagation time* (T_p) or the *time left to initiation* ($T_{i,l}$) are obtained, respectively (Equation (3) and Figure 5).

$$\begin{cases} T_{i,l} = T_i - (T_{survey} - T_{0,agg}), & dCO_2(dCl) < cc \\ T_p = (T_{survey} - T_{0,agg}) - T_i, & dCO_2(dCl) \geq cc \end{cases} \tag{3}$$
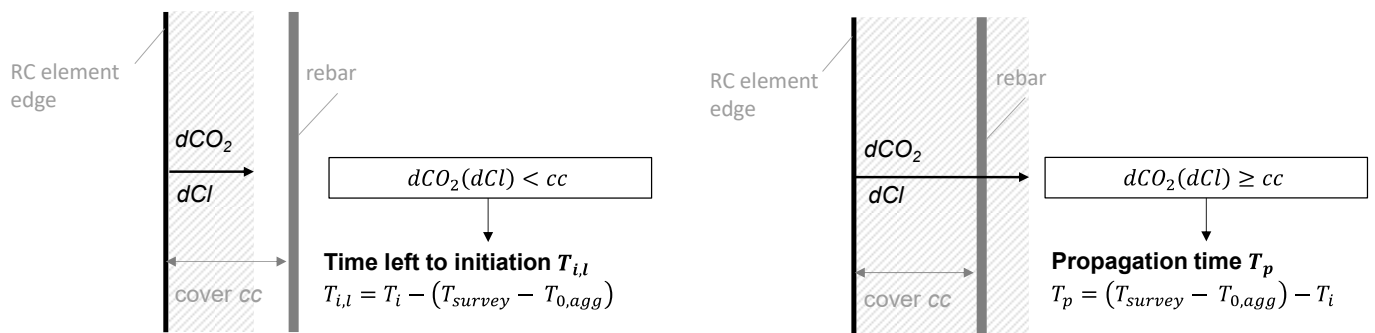
Figure 5. Evaluation of time left to initiation or propagation time according to the procedure proposed in the protocol.

For example, considering a building erected in 1950 (T_0), where the complete removal and repair of the concrete cover was carried out in 1982 ($T_{0,agg}$), and where $dCO_2 = 30$ mm is measured in 2022 (T_{survey}), K would result equal to $K = 30/\sqrt{2022 - 1982} = 4.74$ mm/year$^{1/2}$. If the concrete cover is $cc = 40$ mm, aggressive substances have not yet reached the bars, and the initiation time is $T_i = 40^2/4.74^2 = 71$ years. Accordingly, if exposure conditions remain unchanged, the time left to corrosion initiation is $T_{i,l} = 71 - (2022 - 1982) = 31$ years, which is the time necessary for the aggressive substances to reach the bars from the time of the evaluation. Conversely, if the concrete cover is $cc = 20$ mm, corrosion is probably active, and the initiation time is $T_i = 20^2/4.74^2 = 18$ years, which allows calculating the propagation time (duration of the corrosion attack at the time of evaluation) as $T_p = (2022 - 1982) - 18 = 22$ years.

Starting from the propagation time T_p, an *effective corrosion time T_c* (equal or smaller than the propagation time) should be defined as the time during which significant corrosion rates may have occurred. Indeed, the aggressiveness conditions characterizing the corrosion risk scenario of reference need to be simultaneously present to have values of the corrosion rate which are significant for the structural behaviour. While, for Scenarios 2 and 3, propagation and effective corrosion time may correspond as far as significant corrosion rates are also mostly related to the presence of chlorides in ordinary R.H. conditions, in Scenario 1 (carbonation-induced corrosion in absence of chlorides), significant corrosion rates occur only if high R.H. or contact with water is likely to occur, even if the carbonation front has reached the rebar level. Therefore, it is worth noting whether the exposure conditions have changed in time, for example, due to damage or deterioration of the impermeabilization or of the water collection systems. If past events concerning the structure of interest are not

known, T_c may be assumed as equal to the propagation time (T_p) since conservative results are obtained by adopting a longer duration of the corrosion process.

2.3.2. Corrosion Attack Characteristics

The corrosion attack characteristics are defined in relation to each scenario in order to associate an expected corrosion attack pattern with easily measurable environmental and aggressiveness conditions, thereby providing a preliminary description of a possible corrosion attack. The primary characteristics required to calculate the damage parameters are the *average corrosion rate* (v_{avg}), i.e., the rate of the corrosion attack penetration on the rebars, measured for practical applications in μm/year, and the *maximum-to-average attack ratio* on the bar section (R_p), as proposed also in CONTECVET, 2001 [4] and Berto et al., 2012 [21]. The attack model on the bar section and the attack distribution on the bar length should finally be defined.

1.　Representative values of the average corrosion rate v_{avg}

The corrosion rate is the fundamental information required to estimate the intensity of the attack. Wide ranges of values proposed in Bertolini et al., 2013 [2] (identified with 'B' in Table 6) in relation to the presence of carbonation or chlorides and the level of R.H. were adopted as preliminary intervals of the average corrosion rate characterizing each corrosion risk scenario. Within each scenario, three aggressiveness classes were defined (Ordinary, Aggressive, or Extreme, as described in Table 6), so as to further characterise the values of the corrosion rate in different exposure or humidity conditions. Then, other data from the literature ('M' for Martinez and Andrade, 2009 [22] and 'R' for RILEM, 1996 [23]) were considered to reduce the proposed ranges by adapting to the scenarios' classification the conditions in which they were defined [12]. Values indicated with 'E' in Table 6 were finally estimated by Casprini [12,24] through analyses of corroded bars extracted from existing structures, for which a scenario and an aggressiveness class were identified, and aggressiveness conditions were measured. Finally, some values (named 'REF' in Table 6) are here identified and proposed as the representative values to be adopted for the setting of the equivalent damage parameters, considering all the former data from the literature. The choice of a value included in these ranges should consider that, for all the other conditions set equal, the corrosion rate may increase both for an increasing percentage of chloride and for lower concrete quality; in relation to this, it is crucial to detect zones of poor-quality execution, or honeycomb or cracking due to other causes (conditions from Category C in Table 1). Finally, it should be noted that assuming an average representative value of the corrosion rate v_{avg} is clearly a simplified assumption since it may vary in time due to the conditions in which the attack occurs: for example, while in carbonation-induced corrosion, a corrosion rate increase with time may be triggered by the onset and opening of cracks; in chloride-induced corrosion, once the critical chloride content threshold is reached at the bar level, high corrosion rates may be expected, sometimes also without showing evident cracking.

Table 6. Characteristics of the corrosion attack in each corrosion risk scenario (data adapted from the literature are named as 'B' [2], 'M' [22], and 'R' [23]; data estimated from survey on existing structures are reported with 'E' [12]; final values to be adopted as representative values are indicated with 'REF').

| Scenario		1	2	3
Corrosion Phenomenon		Carbonation-Induced Corrosion	Carbonation-Induced Corrosion + Cl^-	Critical Cl^- Threshold at Rebar Level
Average corrosion rate v_{avg} (μm/year)	**CLASS O** Ordinary R.H. (S2) or marine atmosphere (S3)		B: 2–10 E: 7 (0.20% Cl) 10 (0.34% Cl) **REF: 2–10**	B: 10–50 M: 4 R: 9–40 **REF: 10–50**
	CLASS H High R.H. (S1–S2), chloride airborne (S3)	B: 2–10 M: 2 R: 1–12 E: 7 **REF: 2–10**	B: 10–100 E: 24 (0.27% Cl) **REF: 10–50**	B: 50–100 M: 30 R: 40-80 **REF: 50–100**
	CLASS E Alternation of very wet/dry environment (S1–S2) or zones of water stagnation, splash/tidal zone (S3)	B: 10–100 M: 5 R: 12–50 E: 22–30 **REF: 10–50**	B: 100–200 **REF: 100–200**	B: 100–1000 M: 70 R: 80–120 E: 220 **REF: 100–300**
Maximum-to-average attack ratio R_p		M: 1 E: 1.3–1.9 **REF: 1–2**	E: 3.9–6.2 **REF: 3–7**	M: 10 Tuutti: 4–8 E: 3.2 **REF: 4–10**
Maximum attack type on the bar length		Portion of the bar	Localised deeper attacks	Pitting

2. Maximum-to-average corrosion attack ratio R_p

Once the average corrosion rate v_{avg} is selected and the effective corrosion time T_c is defined, the average corrosion penetration on the rebars can be calculated (Figure 4). A ratio between the maximum and average corrosion attack penetration is then needed to estimate the minimum residual bar cross-section, which often dominates the structural response. In the literature, values ranging between 4 and 8 [25] or 10 [4] are suggested in the case of chloride-induced corrosion (here associated with Scenario 3), which is usually characterised by pitting. On the other hand, the carbonation-induced attack in absence of chloride (Scenario 1) is generally acknowledged to be quite uniform, and such a ratio is often assumed to be equal to 1. Data to be associated with Scenario 2 are not available in the literature, since such a scenario was introduced for the first time in this protocol. Similar to average corrosion rates, preliminary values indicated with 'E' were also estimated in this case from corroded bars analysed through tomographic scans for each scenario [12]: a complete uniform attack was never found, and in Scenario 1, a value ranging between 1–2 was measured; for Scenario 2, values between 3–7 may be preliminary considered, while for Scenario 3 a value of 3.2 was found, since, in this case, a heavy attack was spread along the whole bar length with few more-localised attacks. The literature generally refers to the maximum-to-average attack ratio as 'R'; however, different methods to calculate the residual cross-section, considering either the corrosion penetration or the pit shape, are used to date. For this reason, in this protocol, the maximum-to-average attack ratio is referred to as 'R_p', indicating that only the corrosion penetration (and an equivalent regular shape of the residual section) is considered (see the models in Figure 6). Starting from these characteristics, the average p_{avg} and maximum p_{max} corrosion attack penetration in the bar cross-section can be calculated as in Equations (4) and (5):

$$p_{avg} = v_{avg} \cdot T_c \qquad (4)$$

$$p_{max} = v_{avg} \cdot T_c \cdot R_p \qquad (5)$$
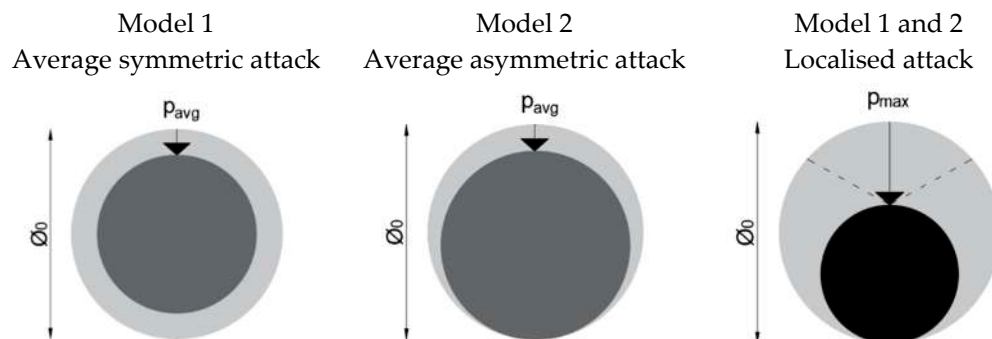
Figure 6. Equivalent average (dark grey) and minimum (black) residual bar cross-section for a given attack penetration.

3. Attack model on the bar section and attack distribution on the bar length

Beyond the quantitative description of the expected corrosion attack, a model of the corrosion attack on the bar section is required to calculate the equivalent damage parameters describing corrosion effects at a sectional level (average and minimum bar residual cross-section and concrete section properties). A summary of the corrosion attack penetration models available in the literature is reported in Casprini, 2021 [12]: for corrosion in absence of chlorides, a regular circular residual cross-section is generally considered, with the corrosion penetration coming either symmetrically from all sides of the bar or mainly from one side (as in the attack model 1 or 2, represented in Figure 6, respectively). In the case of localised corrosion in chloride-contaminated concrete, the minimum cross-section can be estimated considering the shape of the localised attack (pitting corrosion), being the depth of the pit assumed as the maximum penetration; then, the bar cross-section reduction can be computed according to either a hemispherical model of the pit, as proposed by Val and Melchers [26], or by selecting a type of attack morphology following the guidance in the UK Highway Agency BA 51/95 [27]. These methods attempt to define the shape of the localised attack with an accurate geometric model, which may be rarely effective in relation to the variability of corrosion patterns in existing corroding structures. Alternatively, the bar residual cross-section estimate in case of pitting can be simplified by defining an equivalent regular cross-section and neglecting the dimension of the bar surface surrounding the pit [4], as also assumed in this procedure (Figure 6).

As for bond strength and possible ductility reduction, although most of the available formulations are based on the attack penetration at a sectional level, a theoretical modelling [28,29] of these effects and experimental evidence [12] shows that also the attack pattern distribution along the bar length is critical. For this reason, it would be useful to relate simplified model of the attack pattern along the bar length to each scenario: a simplified method is proposed in Casprini, 2021 [12], by defining a single equivalent defect in the bars characterised by the minimum residual cross-section, and a certain length that provides the same bar ductility reduction of the natural corrosion pattern.

2.3.3. Equivalent Damage Parameters

The equivalent damage parameters to be implemented in the structural models at a sectional level are: the average and minimum bar residual cross-sections; the mechanical properties of steel bars; and the geometrical and mechanical concrete section properties. To account for the behaviour of the whole structural element, the residual available ductility of bars, the possible reduction of bond strength between steel and concrete, and, consequently, the possible buckling of longitudinal bars should be considered. In the following, references

to the formulations proposed in the literature to compute these parameters and considerations on their effectiveness in describing corrosion effects are provided. As a first step, the evaluations of the bars' geometrical and mechanical original characteristics, as well as the concrete compressive strength, are required; these characteristics are rarely known when dealing with old RC structures, unless original design or construction documents are available. However, since such information is always necessary to perform structural assessments, these properties are usually estimated by carrying out both non-destructive tests or destructive tests such as tensile tests on bars or compression tests on concrete cores. Other information can be also derived from the construction period and the bar characteristics [30].

1. Average and minimum bar residual cross-section

The average A_{avg} and minimum A_{min} residual cross-sections of bars, which govern their ultimate strength, are the most relevant parameters. Given the average corrosion penetration p_{avg} (Equation (4)), the average attack may be modelled as symmetric or asymmetric (Model 1 and 2 in Figure 6, respectively), as proposed by Andrade [31].

Model 1 may be representative if chlorides are present in the cementitious matrix (a homogeneous reduction from all sides of the bar is expected), while Model 2 is more appropriate for a corrosion attacks due to the presence of water, mainly coming from one side. This choice is left to the engineer carrying out the evaluation; in any case, if the attack type is unclear, Model 1 provides conservative results for the average residual cross-section, provided that for the same corrosion attack penetration, a larger cross-section reduction is obtained (Equation (6)). Considering the minimum residual cross-section, the formulation proposed by Andrade [31] is adopted in both cases, assuming that the maximum corrosion attack penetration (p_{max} from Equation (5)) is equal to the bar diameter reduction (Figure 6 and Equation (7)), and that the area surrounding the localised attack (represented as a dashed line in Figure 6) is neglected for the calculation of the effective minimum residual cross-section.

$$A_{avg,model\ 1} = \frac{\pi(\phi_0 - 2 \cdot p_{avg})^2}{4}$$
$$A_{avg,model\ 2} = \frac{\pi(\phi_0 - p_{avg})^2}{4} \tag{6}$$

$$A_{min} = \frac{\pi(\phi_0 - p_{max})^2}{4} \tag{7}$$

2. Steel bar strength

Agreement among researchers about the occurrence of steel-bar mechanical property deterioration as a consequence of corrosion has not been reached definitively. As for mild steel plain bars, it has been observed that, if the minimum cross-section is considered, the yield and ultimate stresses of corroded bars do not change significantly with respect to the uncorroded one [12,32]. In contrast, mechanical properties may be reduced in bars produced currently, often obtained through thermo-mechanical processes or through the addition of micro-binders; the outer layer of the bar may be characterised by a higher hardness and strength and a lower ductility, with respect to the internal core. Since corrosion mainly affects the outer layer, the actual strength of the corroded bar may be smaller than that of the uncorroded bar [33,34]. Herein, provided that the reduction of the cross-section is considered, and that plain bars are often found in existing structures of main interest for the protocol, yielding and ultimate stresses are assumed to be equal to those of the virgin material, as also assumed in the future version of the Model Code 2020 [29]; however, relationships available in the literature which relate the steel strength reduction to the corrosion level may be adopted [33,35,36], if different types of bars are examined.

3. Concrete section properties

The corrosion of embedded bars also induces effects in the surrounding concrete; in fact, as the bar diameter is reduced by corrosion, metal is transformed into oxides which have a lower density with respect to the original material and, thus, considering the same mass, also have a larger volume. Oxide expansion leads to concrete cracking, changing both the geometrical and mechanical properties of the concrete section. The concrete cross-section can be measured on site in order to detect any variation due to cracking or concrete cover loss. Sounding techniques [9] could help in detecting the presence of cracking or delamination, or in proving that concrete is still sound. Other tests, for example, pulse velocity [9], can be carried out to investigate the integrity of concrete cover. As for cracked concrete, the reduced compressive strength f_c^* is related to the average tensile strain in the transverse direction, which causes longitudinal microcracks, as proposed in Vecchio and Collins [37] and adapted in Coronelli and Gambarova [3] through Equation (8), where k is a coefficient related to bar roughness and diameter (assumed as 0.1 for medium-ribbed bars); ε_{c0} is the strain associated with the maximum compressive stress f_c (uncracked concrete), and ε_1 is the average tensile strain in the cracked concrete (Equation (9)). In this case, b_0 is the section width in the uncracked stage and b_f the section width increased by corrosion cracking, approximated as in Equation (10), where n_{bars} is the number of bars in the top layer (compression zone) and w_{cr} is the total crack width for a corrosion level p (penetration of the corrosion attack), which is evaluated by following Molina et al. [38], as reported in Equation (11); v_{rs} is the ratio of volumetric expansion of the oxides with respect to the virgin material (assumed equal to 2) and $u_{i,corr}$ the opening of each corrosion crack.

$$f_c^* = \frac{f_c}{1 + k \cdot \varepsilon_1 / \varepsilon_{c0}} \tag{8}$$

$$\varepsilon_1 = \left(b_f - b_0 \right) / b_0 \tag{9}$$

$$b_f - b_0 = n_{bars} \cdot w_{cr} \tag{10}$$

$$w_{cr} = \sum_i u_{i,corr} = 2\pi(v_{rs} - 1) \tag{11}$$

Confinement of the concrete core may be disregarded in the analyses of existing corroded structures for mainly two reasons: if corrosion occurred, stirrups are usually the most-exposed type of steel reinforcement, and could experience heavy section loss, being also small-diameter bars, thus leading to a reduction of the confinement effect; moreover, the variability of concrete strength in reinforced concrete structures, and also within the same structural element, is relevant (associated with casting and curing), and the beneficial effect of confinement is not significant, especially for the transverse reinforcement ratios commonly found in existing structures.

4. Residual available ductility

The average ductility of the bar decreases with an increase in corrosion level, and experimental tests [32] show that bar behaviour becomes almost brittle in the case of a localised reduction of the bar cross-section, equal to 50% of the original cross-section. When pitting corrosion occurs, a highly localised strain is induced in the steel at the pit location; when the defect is shallow, the average strain over a finite length of the bar is smaller than the ultimate strain of the virgin material, which is assumed to not change its properties. The formulation proposed in Coronelli and Gambarova [3] is here reported, among other empirical relationships proposed in the literature [33,36]; a reduced ultimate strain (ε'_{su}) is defined through an empirical relationship, starting from the material properties (ultimate and yield strain of the virgin material, ε_{su} and ε_{sy}, respectively) and the pitting corrosion attack level defined as $\alpha_{PIT} = \Delta A_{PIT}/A_0$, where ΔA_{PIT} is the area reduction due to pitting and A_0 the nominal original cross-section. According to the protocol, α_{PIT} can be calculated as $\alpha_{PIT} = (A_0 - A_{min})/A_0$. The proposed relation is based on the assumption that the

ultimate strain is not reduced in the case of uniform attacks, and a complete loss of ductility occurs for a severe reduction of the section (α_{PIT}^{max}). The result is a linear reduction between those thresholds, as described in Equations (12)–(14). Several values of the limit α_{PIT}^{max} were measured in experimental tests, and values ranging from 0.5 [39] to 0.1 [40] are found in the literature.

$$\varepsilon'_{su} = \varepsilon_{su} \qquad\qquad\qquad \alpha_{PIT} = 0 \qquad (12)$$

$$\varepsilon'_{su} = \varepsilon_{sy} + \left(\varepsilon_{su} - \varepsilon_{sy}\right)\left(1 - \frac{\alpha_{PIT}}{\alpha_{PIT}^{max}}\right) \qquad\qquad \alpha_{PIT} < \alpha_{PIT}^{max} \qquad (13)$$

$$\varepsilon'_{su} = \varepsilon_{sy} \qquad\qquad\qquad \alpha_{PIT} = \alpha_{PIT}^{max} \qquad (14)$$

However, this model accounts only for the maximum attack penetration; but, as demonstrated by the results of tensile test on corroded bars [12] and as also proposed in the recent literature [28,29], this is not the only influencing factor. A more refined analytical model should account also for the distribution of the maximum corrosion attack along the bar length. A simplified analytical model aimed at estimating the ductility reduction of the bare bar featuring a single equivalent defect of a certain length with a maximum attack was proposed by the authors in Casprini et al, 2021 [41]; then, since, in existing structures, the corrosion attack distribution on bars is highly variable, and the attack distribution along the bar length is not predictable, it may be useful to relate typical configurations of the natural corrosion patterns to such an equivalent single defect, in order to estimate the residual elongation capacity with the proposed model [12].

5.   Residual bond strength and possible buckling of longitudinal reinforcement

As for residual bond strength, possible change in the failure mode of structural elements, or different locations of critical zones with respect to uncorroded elements, should be accounted for if the corrosion attack involves a large portion of the structural element or the support zones. On the other hand, in the case of very localised attacks, loss of bond is not likely to occur. As for bond strength reduction and buckling of longitudinal rebars, a complete analytical model describing the constitutive law (bond–slip or stress–strain relations) [42–44], or a simplified coefficient accounting for an equivalent reduction of bar strength, respectively, in tension and compression, may be adopted [45,46].

The equivalent damage parameters (EDPs) are preliminarily calibrated to perform sensitivity analyses in order to support the decision-making process for the structure of interest, as presented in Section 3; once the need of including EDPs in the models for structural assessment is evaluated, they are implemented both in analytical models for the estimation of the residual capacity of RC beams [5] and columns [12], or in finite element models [47,48] to assess the global structural behaviour and evaluate the capacity reduction both in terms of base shear and displacement due to corrosion effects. An example of modelling corrosion damage in numerical models is reported in Section 4.

2.4. Step 4—Evaluation of Corrosion Effects on the Structural Behaviour and Actions

The step-by-step procedure of the DEMSA protocol is presented to the user by means of two flow charts (Figures 7 and 8), in which all the results of the previous steps, defined in the previous paragraphs, are included in an ordered manner. The outcomes defined in the last step of the protocol provide information on how to include the corrosion effects in the structural assessment of existing buildings and in the selection and design of the intervention strategy. The reference flow chart is chosen depending on the conditions observed during the visual inspection: in the case of absence of corrosion-induced deterioration (none of the conditions A in Table 2 are detected) the flow chart in Figure 7 is addressed; if signs of corrosion induced-deterioration are visible, the user can skip directly to the procedure in Figure 8. For clarity, instructions are grouped into categories, depending on the type of action needed to obtain the information: on-site surveys and observations (S),

instrumental tests (T), calculations (C), decision-making processes (DM), or qualitative and/or quantitative evaluations through sensitivity analyses (E).
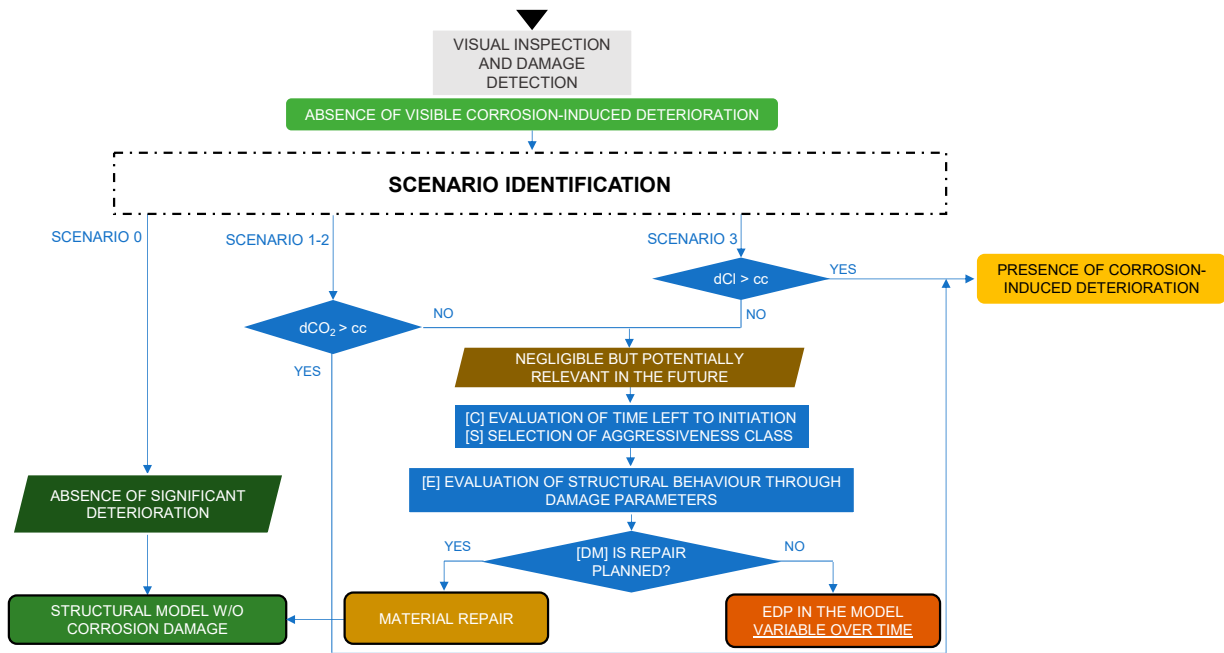
Figure 7. Flow chart to be followed in the case of 'absence of visible corrosion-induced deterioration': starting point and possible outcomes. Type of operations required: (C)—calculations, (S)—surveys, (E1)—qualitative evaluations, (DM)—decision making processes.
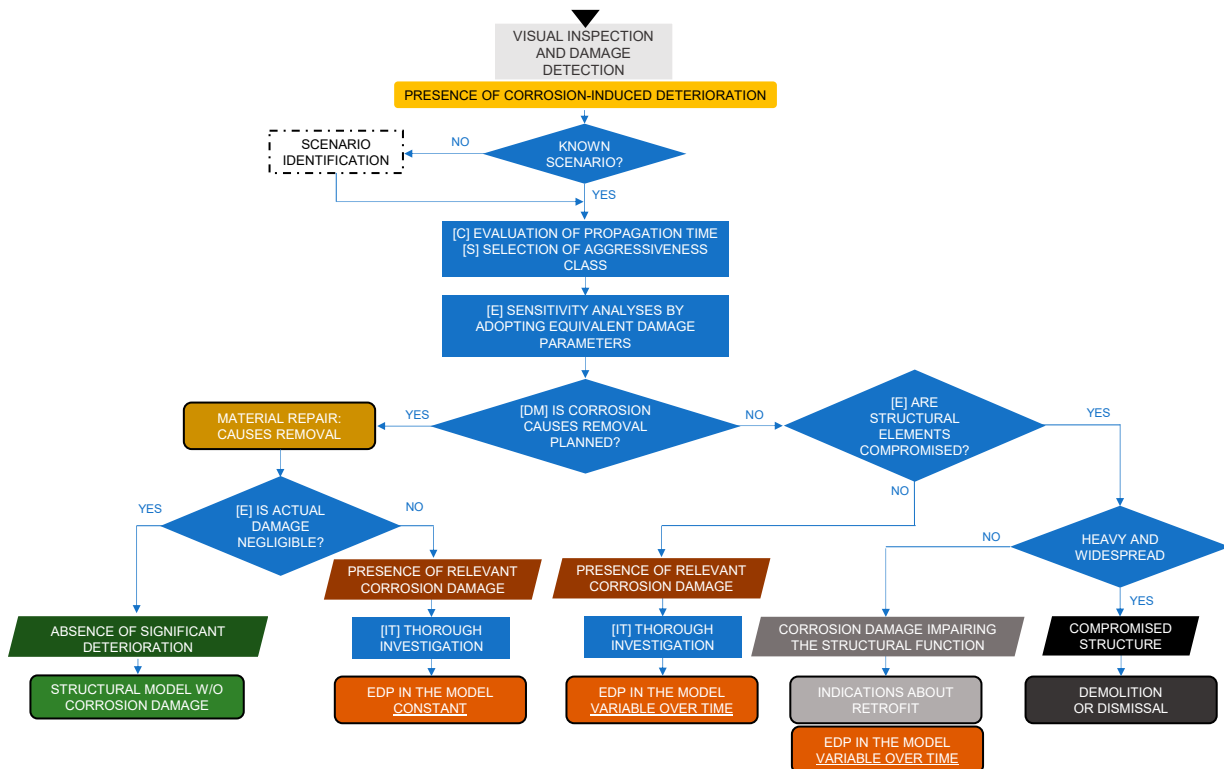
Figure 8. Flow chart to be followed in the case of 'presence of corrosion-induced deterioration'. Type of operations required: (C)—calculations, (S)—surveys, (E2)—quantitative evaluations, (DM)—decision making processes, (IT)—instrumental tests.

2.4.1. Flow Chart 1: Absence of Visible Corrosion-Induced Deterioration

When the visual inspection does not show visible signs of corrosion-induced damage, the protocol enables the determination of one of the following situations: a—corrosion is active but at a low stage (ST3 in Table 1), i.e., without signs on concrete surface; b—corrosion is inactive but may activate in the future (ST0-ST1-ST2 in Table 1); or c—corrosion is inactive because of the lack of conditions to activate, even in the future. Following the flow chart in Figure 7, a possible scenario (0–1–2–3) is defined (according to the scenario identification procedure in Section 2.2); if Scenario 0 is selected, the output 'absence of significant deterioration' is chosen, and the structural analysis can be performed without accounting for corrosion effects ('structural model without corrosion damage'). On the other hand, information about aggressive substance penetration depth and the dimensions of the concrete cover are collated, and two options are possible:

1. The penetration of aggressive substances is deeper than the concrete cover thickness; therefore, they have reached the rebar level (dCO_2 (or dCl) > cc) and the corrosion is likely to be already active. In this case, the second flow chart, 'presence of corrosion-induced deterioration', is used (Figure 8);

2. The penetration of aggressive substances has not reached the rebar level (dCO_2 (or dCl) < cc); thus, the corrosion is not active at the time of the survey, but it could be in the future because the structure belongs to one of those scenarios (1–2–3) in which significant corrosion may occur (deterioration effects are 'negligible but potentially relevant in the future'). In this case, it is possible to estimate the time left until the initiation of corrosion (Equations (1)–(3) and Figure 5), to select a possible aggressiveness class, and to carry out qualitative and/or quantitative evaluations on the expected future structural behaviour, based on the type of damage associated with the corresponding corrosion risk scenario. It is worth mentioning that the DEMSA protocol enables a preliminary evaluation of the corrosion effects, and most of all, of the influence of such effects on the structural behaviour, so that this aspect is not disregarded in the actual practice by structural engineers; if corrosion is then found to be relevant, the support of a corrosion expert is required to perform an accurate detection of the phenomenon and a more detailed definition of the corrosion attack characteristics. Finally, these evaluations can help the user in the decision-making process, to technically support the economic considerations and intervention planning and scheduling. If the action 'material repair', enabling the delay of corrosion initiation, is pursued, repair costs should be accounted for, and then 'structural model without corrosion damage' can be selected; if, instead, such an option is not possible in this phase, evaluations of the future behaviour of the structure should consider 'equivalent damage parameters variable over time' to be implemented in the structural models to plan maintenance operations.

2.4.2. Flow Chart 2: Presence of Visible Corrosion-Induced Deterioration

A second procedure is provided in the case of presence of visible corrosion-induced deterioration or as an output of the previous flow chart (Figure 8); herein, after identifying the possible corrosion risk scenario (1–2–3), propagation time should be calculated, and an aggressiveness class chosen (Ordinary–Aggressive–Extreme) (Figure 5). Accordingly, by selecting possible upper and lower limit values of the corrosion attack characteristics from Table 6, equivalent damage parameters are calculated to perform sensitivity analyses, enabling a first estimate of the effects of corrosion on the structural performance. For example, if, in the worst damage condition (i.e., obtained by implementing the upper values of the attack characteristics), structural behaviour is not affected, the effects of corrosion may be ignored in the structural analysis; on the other hand, if, in the most limited damage condition (i.e., obtained by implementing the lower values of the attack characteristics), structural behaviour is affected, the effects of corrosion should be included in a more detailed structural analysis (and a more accurate analysis of the corrosion phenomena should be performed). Although a more detailed investigation may require

much effort and the help of an expert in corrosion processes, the identification of critical locations of the structural elements, or the knowledge of specific information required to carry out the detailed structural analyses, can help in selecting number and the locations of detailed surveys, enabling a more effective investigation process. The results of the sensitivity analyses support the decision-making process, and several choices can be made about the renovation strategy for the structure of interest. If it is possible to remove those environmental and aggressiveness conditions leading to corrosion, 'material repair' is necessary. Considering the post-repair condition, it is necessary to evaluate whether the existing corrosion damage is negligible, also with the help of the results of the performed sensitivity analyses: in such a case, effects of deterioration are considered negligible for the structural behaviour, and the outputs 'absence of significant deterioration' and 'structural model without corrosion damage' are selected; when it is not, 'constant equivalent damage parameters' (i.e., not varying with time) are implemented in the structural models for further evaluations, in order to account for a reduced actual capacity, or to define an effective structural retrofit.

Since those parameters are implemented in the final structural models, they need to be as accurate as possible. Starting from the preliminary parameters calculated for the sensitivity analyses, a thorough investigation can be carried out in critical locations that may affect the structural behaviour, and that are identified by the preliminary sensitivity analyses, to increase the level of accuracy of the parameter estimation. The concrete cover may be removed in some locations to assess the preservation state of the bars; moreover, the support of a corrosion expert is crucial to perform an accurate assessment of the corrosion conditions. An expert should be in charge of such electrochemical techniques, to correctly interpret the results and to help the structural engineer in obtaining the information required to better calibrate the parameters. Instead, when the removal of the corrosion cause is not possible or not pursued, the sensitivity analyses carried out in the previous step allow evaluations to gauge whether some structural elements are compromised or not reliable, both in the present and in the future. In fact, without removing the causes, the active corrosion process can continue and worsen the structural damage in the future life of the structure. Two options are possible:

1. Structural elements may still be able to perform their structural function. 'Presence of relevant corrosion damage' should be considered in the structural evaluations, also considering its evolution in time. A thorough investigation of the attack characteristics is performed and the output 'equivalent damage parameters variable over time' is thus selected;

2. Structural elements' function is compromised. In this case, if the damage is localised in a few structural elements, those elements could be substituted or retrofitted; or, if damage affects a group of elements, an additional resisting system could be introduced in order to replace the function of the damaged elements, or the load on the structure could be reduced. For example, in the case of seismic retrofit, if a significant reduction in ductility may have occurred at the plastic hinge location on the columns, a new lateral resisting system with shear walls could be introduced, downgrading the columns to the sole role of resisting vertical loads. All these possible actions are grouped into the output 'indications about retrofit'. If instead heavy damage is spread throughout most of the structural elements, 'demolition or dismissal' of the structure should be considered. It is worth noting that such a critical choice is usually also based on economic and social aspects. What needs to be highlighted here is when demolition should be considered because of extended, severe, and irreversible damage of the existing structure.

In the DEMSA protocol, the importance and the strategic role of the examined structure are critical aspects to be considered; interestingly, while, on one hand, significant investment and monitoring programs may be carried out for relevant structures or infrastructures, the problem of corrosion is often disregarded for common RC buildings. The protocol aims at providing agile tools to detect the possible corrosion effects and their relevance

on the structural behaviour also in structures where single simple visual inspections are commonly carried out, and to alert design professionals when an additional support may be required.

3. Application and Validation of the DEMSA Protocol

The validation of the DEMSA protocol procedure was carried out through some real case studies, related to existing structures belonging to different corrosion risk scenarios, in order to evaluate the ability of the protocol to correctly identify the risk of activated corrosion processes, and to effectively estimate the expected corrosion attack in different scenarios [12]. In each structure, after having performed the guided evaluation of the structural condition following the protocol, concrete cover was removed in some locations to assess the actual state of preservation of the structure. Three cases providing different outcomes have been selected to be presented in the following.

3.1. Outcomes 1: Absence of Significant Deterioration

A first example addresses a RC beam belonging to the external colonnade of a building erected in 1960 in Brescia (northern Italy). No signs of deterioration were observed, so the flow chart 'absence of visible corrosion-induced deterioration' (Figure 7) was selected; following the scenario identification procedure (Figure 3), the possible ingress of chloride from the outside of the concrete was excluded, and the chloride content in the concrete matrix was lower than 0.1%. Since the beam was located outdoors, sheltered from rain, the possibility of having wet/dry cycles or high R.H. was excluded. In this case, Scenario 0 can be directly selected, regardless of the carbonation penetration depth, and the outcome 'absence of significant deterioration' is provided. Only for validation purposes was the depth of carbonation measured and compared with the concrete cover dimension; as expected, although carbonation had already reached the rebar level (53 mm against 20 mm), environmental conditions leading to relevant corrosion rates were not present; thus, corrosion can be disregarded in the structural assessment. To confirm this assumption, the concrete cover was removed (Figure 9a) and a bar extracted. The bar was shown to be completely uncorroded and smooth (Figure 9b), as also emphasised by the tomographic scan (Figure 9c) [12].


Figure 9. RC beam of the external colonnade after concrete cover removal (**a**); details of the bar as extracted (**b**) and by tomographic scan (**c**).

3.2. Outcomes 2: Indications about Retrofit

The interesting case of a school building (from 1959) in northern Italy is described herein. At the time of the survey (year 2020) the building was under investigation for the preliminary design of a seismic retrofit intervention. Although an apparently good state of preservation was initially observed, some longitudinal cracks were detected at the base of almost 10% of the school's columns (Figure 10a). Following the protocol guidance, the flow chart 'presence of corrosion-induced deterioration' (Figure 8) was selected. The scenario identification procedure (Figure 3) was first carried out. The possible ingress of chloride from the outside of the concrete was excluded in the interior of the school; therefore, the chloride content in the concrete matrix was measured in two columns by drilling some concrete powder and performing chemical standard potentiometric titration [17].

The resulting chloride content was 0.20% (column SB1) and 0.34% (SB2), with respect to cement weight. A possible Scenario 2 and aggressiveness class 'Ordinary' was thus selected. The comparison between the cover thickness and the carbonation depth showed that carbonation had already reached the rebar level (average carbonation depth of 95 mm against 30 mm of concrete cover). Accordingly, the propagation time was estimated (almost 50 years with respect to the 61 years of structure age). The effective corrosion time was considered equal to the propagation time, with corrosion being probably caused by the presence of chloride in the matrix since construction. From a qualitative point of view, such a corrosion attack could lead to a reduction in the bars' cross-section (with the possible presence of localised deep attacks) and in the ductility of the steel bars; to the cracking of the concrete surrounding the bar; to the loss of bond between bars and concrete; and, consequently, to the possible buckling of longitudinal rebars. Since the location of damage was mainly present in the lower end of the columns, in terms of seismic vulnerability, such damage cannot be disregarded.

(a) **(b)** **(c)** **(d)**
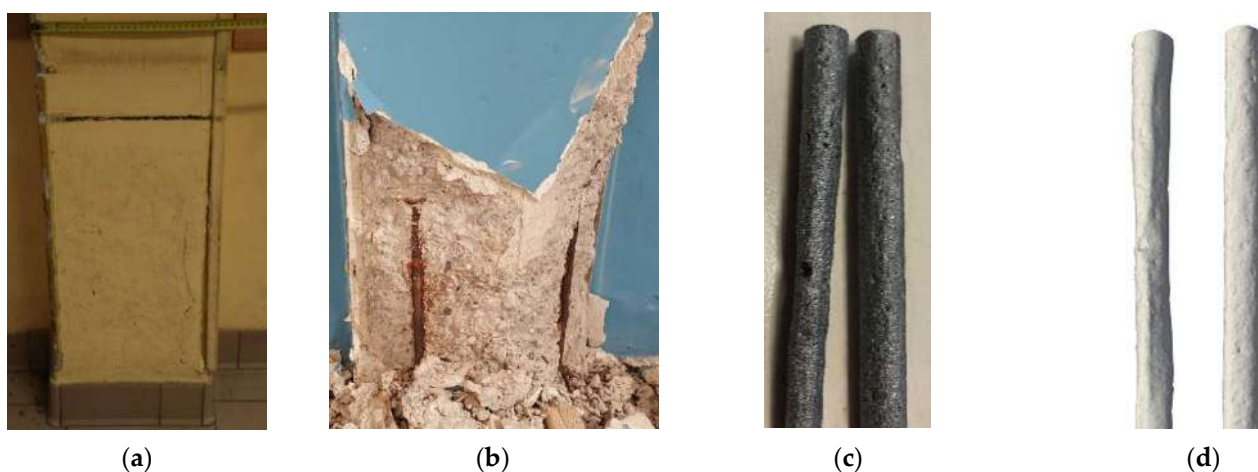
Figure 10. RC columns from the school building: longitudinal cracking (**a**); corroded bars observed after concrete cover removal (**b**); details of the extracted bars after cleaning (**c**) and by tomographic scan (**d**). (Pictures refer to different columns of the same building.)

As for quantitative evaluation, an average corrosion rate range of 2–10 μm/year was selected from Table 6. Assuming the worst damage condition, a corrosion penetration of 500 μm (10 μm/year for 50 years) was estimated. By adopting Model 1 for the average cross-section reduction (Figure 6), the original bar diameter (10 mm) may present an average reduction of 1 mm. It is worth noting that, in this attack type, the maximum penetration is more relevant because localised attacks may have occurred due to chlorides. A maximum-to-average attack ratio equal to 7 may be considered. This means that, in some points of the bar, a corrosion penetration of 3.5 mm may have occurred, corresponding to the diameter reduction of the minimum cross-section (Figure 6). Considering this preliminary estimation, an average and minimum residual cross-section equal to 81% and 42% of the original one may be present, respectively. As for the seismic behaviour, such a reduction of section and possible reduction of ductility is not negligible. Assuming that the cause of corrosion would have not been removed (due to the presence of chlorides spread throughout the concrete matrix), it can be said that in the actual condition, and in the future life of the structure, RC columns, being not originally designed to withstand horizontal actions, cannot be conceived as part of the lateral force-resisting system. (Figure 10). Thus, given that corrosion damage impairing the structural function was observed in several columns, while the rest of the structural system showed a fair state of preservation, a downgrade of the structural role of the columns and the addition of shear resistant walls withstanding the whole seismic action were considered; this way, the columns would be only subjected to static loads.

The investigation on the school building was also used for validation purposes. The concrete cover was removed in some of the columns, and the presence of an activated corrosion attack on the bars was confirmed (Figure 10b). Furthermore, a bar was extracted from each analysed column, and the residual average (A_{avg}) and minimum (A_{min}) cross-section were measured through tomographic scans (Figure 10c,d). Starting from these data, the average corrosion rate and the maximum-to-average attack ratio were also estimated (results are reported in Table 7).

Table 7. Bars' average and minimum residual cross-section, with respect to the original one, and corrosion attack characteristics estimated by processing the results of tomographic scans of bar SB1–SB2 [12].

Column	A_{avg}/A_0 (%)	A_{min}/A_0 (%)	K (mm/years$^{1/2}$)	T_i (years)	T_c (years)	v_{avg} (μm/year)	R_p
SB1	86.8	72.3	12.8	7.5	53.5	6.6	6.12
SB2	83.2	57.4	11.5	15.2	45.8	9.4	4.83

Good agreement was found between the expected and measured attacks. This example highlights some fundamental results: a very strong attack can be found also in structures showing an apparently good state of preservation, and this can be due to the high porosity of concrete which prevents corrosion products' expansion to result in external cracking; corrosion effects are critical for the structural behaviour and need to be necessarily considered in the structural assessment and design of the retrofit solution. Moreover, the proposed procedure may be effective in detecting the risk of activated corrosion, and the attack characteristics related to the scenarios allow a preliminary estimates of the expected attack.

3.3. Outcomes 3: Definition of Equivalent Damage Parameters Variable over Time

In the previous examples, the effects of corrosion were either negligible for the structural behaviour, or conversely, so heavy as to provide major indications about the intervention strategy. In many intermediate conditions, further evaluations are required. This is the case of the RC elements of a private car park annexed to a residential building from the early 1970s in Milan, northern Italy. During the condition survey, damp spots on the floor intrados were observed, revealing a problem of water infiltration from the garden above the car park. In addition, a few longitudinal cracks and/or delamination were detected in many beams. Following the protocol guidance for a beam where internal delamination was detected, the flow chart 'presence of corrosion-induced deterioration' (Figure 8) was selected. The scenario identification procedure (Figure 3) was first carried out: because the possible ingress of chloride from the outside of the concrete was excluded, the chloride content in the concrete matrix was measured, resulting in 0.27% with respect to cement weight [17]. Scenario 2 was confirmed for the beam under investigation, and aggressiveness class 'High' was chosen because of the presence of water infiltration from the garden above and the scarce lighting and ventilation since the building's construction. The comparison between the cover thickness and the carbonation depth showed that carbonation had already reached the rebar level (average carbonation depth of 39 mm against 15 mm of concrete cover). Accordingly, the propagation time was estimated (almost 43 years with respect to the 50 years of structure age). The effective corrosion time was considered equal to the propagation time since the infiltration problems were present in the car park since construction. For a quantitative evaluation of the corrosion effects, an average corrosion rate range of 10–50 μm/year was selected from Table 6. Assuming the worst damage condition, a corrosion penetration of 2.15 mm (50 μm/year for 43 years) was estimated. By adopting Model 1 for the average cross-section reduction (Figure 6), the original bar diameter (20 mm) may present an average reduction of 4.3 mm. A maximum-to-average attack ratio equal to 5 may be considered; in this case, a mean value between those of the reference is selected, since the attack is mainly dominated by the presence of water. This means that, in some points of the bar, a corrosion penetration of 10.8 mm may have occurred,

corresponding to the diameter reduction at the minimum cross-section. Considering this preliminary estimation, an average and minimum residual cross-section equal to 62% and 21% of the original one may be present, respectively. If, following the same procedure, the lower value of the possible corrosion rate range is assumed (10 μm/year for 43 years and R_p = 5), an average and minimum residual cross-section equal to 92% and 80% of the original one may be present, respectively.

Although, in both cases, the residual capacity of beams may be strongly affected by corrosion, a more accurate evaluation of the corrosion damage with the support of a corrosion expert is required for this structure, to reduce the uncertainty of the prediction.

For validation purposes, the concrete cover was removed in some of the beams (Figure 11a), and the presence of an activated corrosion attack on the bars was confirmed. Furthermore, a bar was extracted from the analysed beam and the residual average (A_{avg}) and minimum (A_{min}) cross-section were measured through tomographic scans (Figure 11b,c). Starting from these data, the average corrosion rate and the maximum-to-average attack ratio were also estimated (results are reported in Table 8).

(a)

(b)

(c)

Figure 11. RC beam from the car park after concrete cover removal (**a**); details of the bar as extracted (**b**) and by tomographic scan (**c**).

Table 8. Bar's average and minimum residual cross-section, with respect to the original one, and corrosion attack characteristics estimated by processing the results of tomographic scans of bar RB1 [12].

Column	A_{avg}/A_0 (%)	A_{min}/A_0 (%)	K (mm/years$^{1/2}$)	T_i (years)	T_c (years)	v_{avg} (μm/year)	R_p
RB1	89.9	80.6	5.7	7	43	24	3.96

When a structural retrofit is not immediately required, such as in the latter example, the definition of the equivalent damage parameters is fundamental to derive a curve of the structural performance over time, which is used as a tool to define the retrofit intervention scheduling and timing, once a reference acceptable limit condition is defined (in the example in Figure 12, the achievement of 85% of the initial capacity is considered).

Several strategies can be carried out (Figure 12): if possible, repair techniques to stop the corrosion process and its future activation can be undertaken at the time of the survey (A) or at the achievement of a given limit state (B). If structural retrofit is not considered, an equivalent damage parameter describing the residual capacity of the structure should be implemented in any further modelling of the structural behaviour. It can be also decided to perform a structural retrofit (for example, the integration of bars or other strengthening methods) to restore the initial capacity (C) or a higher one (D–E–F). In this case, the new time left to corrosion initiation may depend on the concrete cover characteristics or dimensions. If aggressiveness conditions are not changed, it may be expected that future deterioration follows the same trend as the original curve (D); on the other hand, some mitigation measures for future corrosion attacks, such as the reduction of environmental R.H., may be carried out in order to either reduce the curve slope (E) or to finally stop the future activation of corrosion (F). The example reported herein, as a proof of the concept, shows

the importance of having a tool to perform evaluations of the structural behaviour over time when affected by corrosion damage effects. It also emphasises the need of further collaboration between structural engineers and material and corrosion experts to conceive, plan, and carry out repair techniques that are able to obtain the maximum beneficial effect for both maintenance costs over service life, and structural behaviour expected in the as-is condition and after the retrofit intervention.
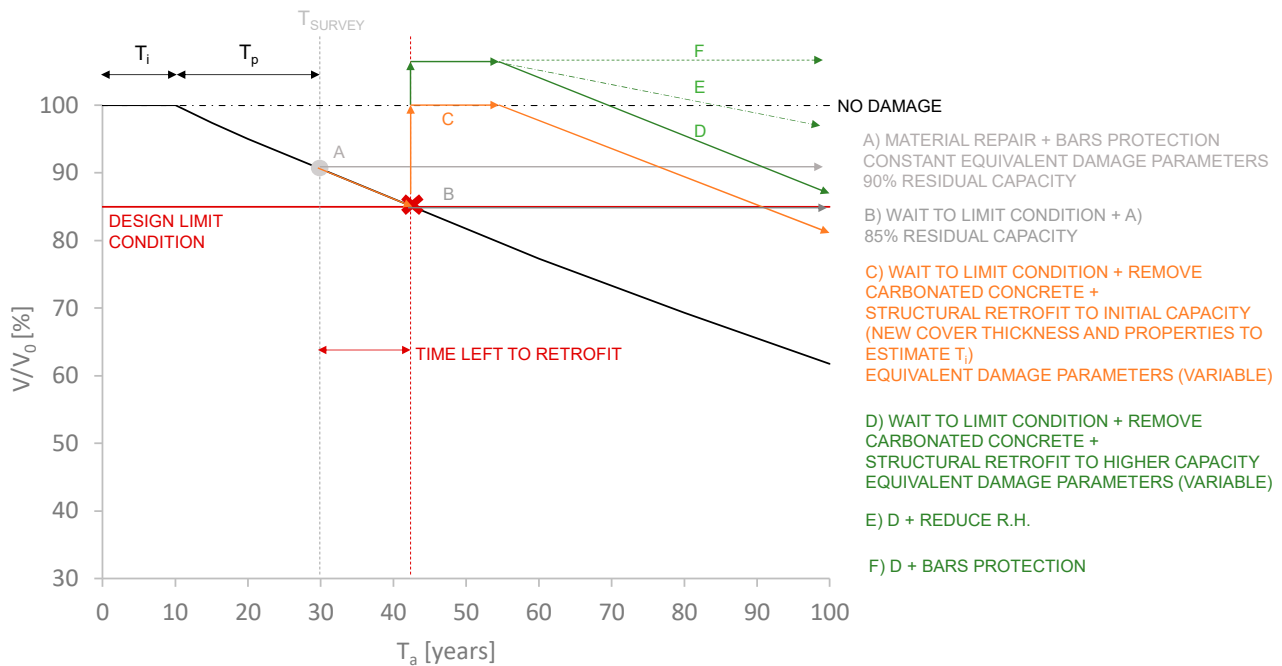

Figure 12. Example of the implementation of the predictive models in the assessment of the residual life of existing structures and in the maintenance schedule and planning.

4. Implementation of EDP in the Structural Modelling

As a proof of the concept, an example of structural modelling, including the equivalent damage parameters, is reported in this section. Simplified corrosion patterns representing natural corrosion damage associated with the buildings described in Section 3 are implemented on a single bay frame (Figure 13). Non-linear static analyses (by means of fibre modelling, adopting the software MidasGen [49]) are carried out to evaluate the residual capacity of the frame in terms of base shear and top displacement; the reference frame features two columns (30×30 cm; H = 3.15 m; $4\phi16$ as reinforcement) and a beam (65×23 cm; L = 4 m; $3\phi16$ and $4\phi12$ as top and bottom reinforcement, respectively). Some assumptions are considered in the model (described in detail in Casprini [12]): the Park model and the Nagoya Highway Corporation model are adopted for steel (f_y = 360 MPa; f_t = 540 MPa) and concrete materials (f_c = 25 MPa; ε_{cu} = 0.4%), respectively [49]; a possibly beneficial confinement effect for concrete material is neglected, and the compressive strength of concrete is reduced in the concrete cover according to the corrosion level, as proposed in Equations (8)–(11) [3]; failure is assumed to occur for flexure and the effects of corrosion on bond strength and possible buckling of longitudinal rebars are neglected in this preliminary phase. Gravity loads of 19 kN/m distributed on the beam and 500 kN acting on the columns are modelled. As for the corrosion pattern of the school building, the worst condition for Scenario S2O is assumed as detailed in Section 3.2 (T_c = 50 years, Model 1 for bar average cross-section reduction, v_{avg} = 10 μm/year, R_p = 7), while for the car park in Scenario S2H, an intermediate condition is assumed (T_c = 43 years, Model 1 for bar average cross-section reduction, v_{avg} = 30 μm/year, R_p = 5). A simplified method (further detailed in Casprini et al. [41]) is here adopted to model an uneven corrosion attack pattern by means of a simplified one: the average attack ('avg') is modelled in the whole

corroded elements, except for a portion where the maximum attack ('max') is introduced. This portion is defined as a single 'equivalent defect', which is characterised by a chosen length, associated with the scenario of interest and the aggressiveness of the attack (in this case, 15 cm for the school and 40 cm for the car park).
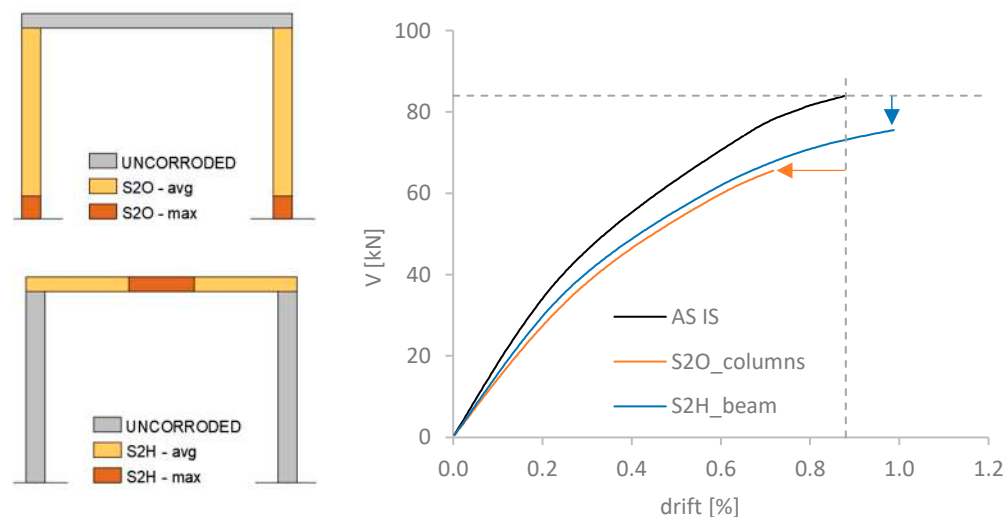
Figure 13. Capacity curves of a 2D RC frame in the as-is condition, with a corrosion pattern associated with the school building (S2O_columns) and with the private car park (S2H_beam) described in Section 3. The curves are interrupted in correspondence with a brittle failure of the elements.

A global stiffness reduction is observed in the corroded structures, since the reduction of the concrete cover compressive strength to account for cracking at the columns base entails a reduced elasticity modulus of the concrete material. While the corrosion of the beam results in a reduced shear capacity of the reference RC frame (89%, with respect to the original one), the degradation of the columns with the defect localised at the base entails a reduction also in the displacement capacity (80%, with respect to the original one). The constitutive relationships adopted for the concrete and steel result in a moment–curvature relationship characterised by brittle failure in the critical sections of the elements; accordingly, no post peak resistance is observed.

The seismic vulnerability of the examined structures significatively increases due to corrosion, and it is expected to increase even more in the future life of the structures if the causes triggering and sustaining the corrosion processes are not removed. A wider sensitivity analysis on the structural response can be performed by varying the characteristics of the corrosion attack (for example, in terms of corrosion rate, defect length, spatial distribution of the maximum attacks, or effective corrosion time) within the possible range of values from the scenarios. The structural response in each condition allows for identifying the expected best- and worst-case scenarios; accordingly, if necessary, a thorough diagnostic campaign can be planned to reduce the uncertainties and to collect such data which are significant for the structural response required to calibrate the structural model.

The application of the protocol procedure to the modelling and assessment of real buildings would highlight even more the potentialities of the proposed procedure; this paper is aimed at providing a comprehensive description and validation of the protocol, while single aspects which need further research are under investigation, and the application to more complex case studies is the object of ongoing research. In this context, this example on a single-bay frame highlights both the importance of modelling corrosion damage in the structural assessment, and of how the defined simple parameters may be used for a preliminary estimate of the change in structural behaviour in different environmental conditions; disregarding possible corrosion effects, especially when deterioration signs are not clearly visible, but corrosion is active, may lead to wrong predictions of the actual behaviour and, consequently, to an ineffective retrofit intervention.

5. Concluding Remarks and Research Needs

A simplified protocol for practical applications of diagnosis and assessment of existing RC structures has been presented in this paper, which allows for detecting whether corrosion effects may be relevant for the structural behaviour, starting from easily measurable environmental and aggressiveness conditions related to some corrosion risk scenarios. Starting from this hypothesis, corrosion-induced damage is estimated, through equivalent damage parameters, to be included in the structural models, such as the average and minimum residual bar cross-sections and the concrete section residual properties. The engineer is, therefore, guided throughout the whole assessment process, from the on-site inspection to the evaluation of the structural performance, addressing both the residual capacity of single structural elements by means of simplified analytical models, and the global behaviour by modelling simplified corrosion patterns with numerical models. The main developments introduced in the protocol with respect to the current assessment practice are summarised in the following, along with those aspects requiring further investigation:

- The protocol user is guided through a series of consecutive steps which allow a simplified evaluation of whether corrosion damage may be present and which type of attack may be expected. To this end, the user is guided to the design of the diagnostic campaign, and to the definition of the suitable in situ measurements tests, which are necessary to detect the actual risk of corrosion. The already-available instrumental tests are integrated within the protocol; on the other hand, the need of developing a rapid test enabling the evaluation of the presence and amount of chloride in concrete is emphasised;

- Corrosion risk scenarios are introduced to group together all environmental conditions leading to similar corrosion attacks, described through the corrosion attack characteristics. Such characteristics, especially the average corrosion rate and the maximum-to-average attack ratio, should be further detailed to reduce the proposed ranges. More correlations among environmental aggressiveness conditions and effective corrosion damage are thus required;

- Simplified equivalent damage parameters are calibrated based on the previous collected input data. The models adopted in the protocol for the evaluation of the bar residual cross-section are those acknowledged as the most practical and straightforward; despite that more refined modelling of the localised attack is often proposed in the literature, it requires a level of accuracy which does not match the reduced feasibility of in-field measurements. As for the other parameters, also simplified attack pattern distributions along the bar length may be provided in the future in relation to each scenario;

- Along all its steps, the protocol maintains focus on the effects of deterioration on the structural behaviour of the building, in relation to the assessment of the structure and the choice of the suitable renovation strategy.

Finally, it should be emphasised that cooperation among different fields of expertise is essential to provide effective tools for the evaluation of corrosion effects and of their impact on the structural performance and expected service life of existing structures. The DEMSA protocol is conceived as a rationalised and flexible procedure, in which new research achievements, such as more refined corrosion attack characteristics, more accurate formulations of the equivalent damage parameters, or advanced diagnostic techniques, can be easily implemented, thereby enabling progressive updates for each single step of the protocol.

References

1. Marini, A.; Passoni, C.; Belleri, A.; Feroldi, F.; Metelli, G.; Preti, M.; Giuriani, E.; Riva, P.; Plizzari, G. Combining seismic retrofit with energy refurbishment for the sustainable renovation of RC buildings: A proof of concept. *Eur. J. Environ. Civ. Eng.* **2017**, *10*, 1080. [CrossRef]
2. Bertolini, L.; Elsener, B.; Pedeferri, P.; Redaelli, E.; Polder, R. *Corrosion of Steel in Concrete—Prevention, Diagnosis, Repair*; Wiley VCH: Weinheim, Germany, 2013.
3. Coronelli, D.; Gambarova, P.G. Structural assessment of corroding R/C beams: Modelling guidelines. *ASCE J. Struct. Eng.* **2004**, *130*, 1214–1224. [CrossRef]
4. IN30902I. CONTECVET. A Validated User Manual for Assessing the Residual Life of Concrete Structures. DG Enterprise, CEC. 2001. Available online: https://www.ietcc.csic.es/en/ (accessed on 26 April 2022).
5. Coronelli, D. Resistance of corroded RC beams: Extending fib Model Code 2010 models. *Struct. Concr.* **2020**, *21*, 1747–1762. [CrossRef]
6. *EN 1998-3*; Eurocode 8 Design of Structures for Earthquake Resistance. CEN: Brussels, Belgium, 2005.
7. FIB. *Fib Model Code for Concrete Structures, 2010*; Wilhelm Ernst & Sohn, Wiley: Berlin, Germany, 2013.
8. Passoni, C.; Marini, A.; Belleri, A.; Menna, C. Redefining the concept of sustainable renovation of buildings: State of the art and LCT-based design framework. *Sustain. Cities Soc.* **2021**, *64*, 102519.
9. ACI Committee 222. *ACI 222R-19: Guide to Protection of Reinforcing Steel in Concrete against Corrosion*; ACI: Farmington Hills, MI, USA, 2019.
10. Coppola, L.; Buoso, A. *Il Restauro Dell'architettura Moderna in Cemento Armato*; Ulrico Hoepli Editore: Milano, Italy, 2015.
11. Andrade, C. Propagation of reinforcement corrosion: Principles, testing and modelling. *Mater. Struct.* **2019**, *52*, 2. [CrossRef]
12. Casprini, E. A Protocol for the Assessment of Corrosion Effects in RC Structures in a Life Cycle Engineering Framework. Ph.D. Thesis, University of Bergamo, Dalmine, Italy, 2021.
13. *EN 206:2013*; Concrete-Specification, Performance, Production and Conformity. CEN: Brussels, Belgium, 2013.
14. Çağatay, I.H. Experimental evaluation of buildings damaged in recent earthquakes in Turkey. *Eng. Fail. Anal.* **2005**, *12*, 440–452. [CrossRef]
15. *EN 14630*; Products and Systems for the Protection and Repair of Concrete Structures—Test Methods—Determination of Carbonation Depth in Hardened Concrete by the Phenolphtalein Method. CEN: Brussels, Belgium, 2006.
16. Felicetti, R. Improved Procedure for the Analysis of Construction Materials and Device to Implement This Procedure. Italian Patent Application MI2009A 001073, 17 June 2009.
17. *EN 14629*; Products and Systems for the Protection and Repair of Concrete Structures—Test Methods—Determination of Chloride Content in Hardened Concrete. CEN: Brussels, Belgium, 2007.
18. Herald, S.E.; Henry, M.; Al-Qadi, I.L.; Weyers, R.E.; Feeny, M.A.; Howlum, S.F.; Cady, P.D. *Condition Evaluation of Concrete Bridges Relative to Reinforcement Corrosion. Volume 6: Method for Field Determination of Total Chloride Content*; Strategic Highway Research Program, National Research Council: Washington, DC, USA, 1993.
19. Jackson, D.R.; Soh, F.W.; Scannel, W.T.; Sohanghpurwala, A.A.; Islam, M. Comparison of chloride content analysis results using the AASHTO T260 test method and two field test kits. In Proceedings of the Corrosion95. The NACE International Annual Conference and Corrosion Show, Houston, TX, USA, 1 September 1995.
20. Collepardi, M.; Marcialis, A.; Turriziani, R. Penetration of chloride ions in cement pastes and in concretes. *J. Am. Ceram. Soc.* **1972**, *55*, 534–535. [CrossRef]

21. Berto, L.; Saetta, A.; Simioni, P. Structural risk assessment of corroding RC structures under seismic excitation. *Constr. Build. Mater.* **2012**, *30*, 803–813. [CrossRef]
22. Martínez, I.; Andrade, C. Examples of reinforcement corrosion monitoring by embedded sensors in concrete structures. *Cem. Concr. Compos.* **2009**, *31*, 545–554. [CrossRef]
23. RILEM. *Durability Design of Concrete Structures*; Report No. 14; E & FN Spon: London, UK, 1996.
24. Casprini, E.; Passoni, C.; Marini, A.; Bartoli, G.; Gastaldi, M.; Riva, P. Effects of corrosion on the structural behaviour of existing structures: Corrosion Risk Scenarios and equivalent parameters. In *Capacity Assessment of Corroded Reinforced Concrete Structures, Proceedings of the Fib CACRCS Days 2020, Online Event, 1–4 December 2020*; International Federation for Structural Concrete: Lausanne, Switzerland, 2020.
25. Tuutti, K. *Corrosion of Steel in Concrete*; Swedish Cement and Concrete Research Institute: Stockholm, Sweden, 1982.
26. Val, D.V.; Melchers, R.E. Reliability of deteriorating RC slab bridges. *J. Struct. Eng.* **1997**, *123*, 1638–1644. [CrossRef]
27. UK Highways Agency BA 51/95. *The Assessment of Concrete Structures Affected by Steel Corrosion*; The Stationery Office Ltd.: London, UK, 1995.
28. Chen, E.; Berrocal, C.G.; Fernandez, I.; Lofgren, I.; Lundgren, K. Assessment of the mechanical behaviour of reinforcement bars with localised pitting corrosion by Digital Image Correlation. *Eng. Struct.* **2020**, *219*, 110939. [CrossRef]
29. Walrawen, J. Significance of reinforcement corrosion for modelling the behaviour of existing concrete structures. In Proceedings of the CACRCS Days 2020, Online Event, 1–4 December 2020.
30. Verderame, G.M.; Ricci, P.; Esposito, M.; Sansiviero, F.C. Le Caratteristiche Meccaniche Degli Acciai Impiegati Nelle Strutture in C.A. Realizzate dal 1950 al 1980. In Proceedings of the Atti del XXVI Convegno Nazionale AICAP Le Prospettive di Sviluppo Delle Opere in Calcestruzzo Strutturale Nel Terzo Millennio, Padova, Italy, 19–21 May 2011.
31. Andrade, C. Approach to the residual strength of steel bars due to corrosion. In Proceedings of the Fib CACRCS Days 2021, Online Event, 30 November–3 December 2021.
32. Palsson, R.; Mirza, M.S. Mechanical response of corroded steel reinforcement of abandoned concrete bridge. *ACI Struct. J.* **2002**, *99*, 157–162.
33. Imperatore, S.; Rinaldi, Z.; Drago, C. Degradation relationship for the mechanical properties of corroded steel rebars. *Constr. Build. Mater.* **2017**, *148*, 219–230. [CrossRef]
34. Apostolopoulos, C.A. The influence of corrosion and cross-section diameter on the mechanical properties of B500C steel. *J. Mater. Eng. Perform.* **2008**, *18*, 190–195. [CrossRef]
35. Du, Y.G.; Clark, L.A.; Chan, A.H.C. Residual capacity of corroded reinforcing bars. *Mag. Concr. Res.* **2005**, *57*, 135–147. [CrossRef]
36. Cairns, J.; Plizzari, G.A.; Du, Y.; Law, D.W.; Franzoni, C. Mechanical properties of corrosion-damaged reinforcement. *ACI Mater. J.* **2005**, *102*, 256–264.
37. Vecchio, F.; Collins, M.P. The modified compression field theory for reinforced concrete elements subjected to shear. *Proc. ACI* **1986**, *83*, 219–231.
38. Molina, F.J.; Alonso, C.; Andrade, C. Cover cracking as a function of rebar corrosion. II: Numerical model. *Mater. Struct.* **1993**, *26*, 532–548. [CrossRef]
39. Cairns, J.; Millard, S. Section 13:2: Reinforcement corrosion and its effect on residual strength of concrete structures. In Proceedings of the 8th International Conference on Structure Faults and Repair, Edinburgh, UK, 1 January 1999.
40. Castel, A.; Francois, R.; Arliguie, G. Mechanical behavior of corroded reinforced concrete beams. II: Bond and notch effects. *Mater. Struct.* **2000**, *33*, 545–551. [CrossRef]
41. Casprini, E.; Passoni, C.; Marini, A.; Bartoli, G. Modelling corrosion effects in reinforced concrete Structural members through equivalent damage parameters. In *Capacity Assessment of Corroded Reinforced Concrete Structures, Proceedings of the Fib CACRCS Days 2021, Online Event, 30 November–3 December 2021*; International Federation for Structural Concrete: Lausanne, Switzerland, 2021.
42. Blomfors, M.; Zandi, K.; Lundgren, K.; Coronelli, D. Engineering bond model for corroded reinforcement. *Eng. Struct.* **2018**, *156*, 394–410. [CrossRef]
43. Coronelli, D.; Francois, R.; Dang, H.; Zhu, W. Strength of corroded RC beams with bond deterioration. *J. Struct. Eng.* **2019**, *145*, 04019097. [CrossRef]
44. Imperatore, S.; Rinaldi, Z. Experimental behavior and analytical modeling of corroded steel rebars under compression. *Constr. Build. Mater.* **2019**, *226*, 126–138. [CrossRef]
45. Tapan, M.; Aboutaha, R.S. Effect of steel corrosion and loss of concrete cover on strength of deteriorated RC columns. *Constr. Build. Mater.* **2011**, *25*, 2596–2603. [CrossRef]
46. Campione, G.; Cannella, F.; Cavaleri, L.; Ferrotto, M.F. Moment-axial force domain of corroded R.C. columns. *Mater. Struct.* **2017**, *50*, 21. [CrossRef]
47. Dizaj, E.A.; Madandoust, R.; Kashani, M.M. Probabilistic seismic vulnerability analysis of corroded reinforced concrete frames including spatial variability of pitting corrosion. *Soil Dyn. Earthq. Eng.* **2018**, *114*, 97–112. [CrossRef]
48. Berto, L.; Caprili, S.; Saetta, A.; Salvatore, W.; Talledo, D. Corrosion effects on the seismic response of existing RC frames designed according to different building codes. *Eng. Struct.* **2020**, *216*, 110397. [CrossRef]
49. Midas GEN. *Software User Manual*; MIDASoft Inc.: New York, NY, USA, 2020.